國立交通大學

生物科技研究所

碩 士 論 文

Arthrobacter globiformis 組織胺氧化酵素受質特異性研究

Research of Substrate Specificity of
Arthrobacter globiformis **Histamine Oxidase**

研 究 生：楊政剛
指導教授：袁俊傑 博士

中 華 民 國 九 十 三 年 七 月

Arthrobacter globiformis 組織胺氧化酶受質特異性研究

Research of Substrate Specificity of *Arthrobacter globiformis* Histamine Oxidase

研 究 生：楊政剛　　Student：Jen-Gong Yang

指導教授：袁俊傑 博士　　Advisor：Dr. Chiun-Jye Yuan

國 立 交 通 大 學

生 物 科 技 研 究 所

碩 士 論 文

A Thesis
Submitted to Department of Biological Science and Technology
National Chiao Tung University
in partial Fulfillment of the Requirements
for the Degree of
Master
in
Biological Science and Technology
July 2004

Hsinchu, Taiwan, Republic of China

中華民國九十三年七月

Arthrobacter globiformis 組織胺氧化酵素受質特異性研究

研 究 生：楊政剛　　　　　　　　　　　　指導教授：袁俊傑　博士

國立交通大學生物科技研究所碩士班

中文摘要

含銅胺類氧化酵素 [EC1.4.3.6] 廣泛存在於細菌、酵母菌、黴菌、動物及植物界。此類酵素藉由氧化去胺作用分解一級胺類而產生醛類，氨和過氧化氫。不同來源的胺類氧化酵素彼此之間的受質特異性具有很大的差異。關於受質特異性上的差異一直是研究上的重要課題，為了釐清其中的差異，我們利用AGHO此株酵素來研究，一系列在結構上相似的aromatic amines，在其aliphatic chain 的長度及aromatic ring上一些官能基的修飾，探討其對受質特異性的影響。從其中的kinetic analysis比較中，實驗結果顯示隨著aromatic amines上帶有胺基的aliphatic chain長度增加，K_m會隨之下降。而在一些結構相似的aromatic amine研究之中，發現aromatic ring的hydropathy會影響substrate specificity (K_{cat}/K_m)。

之前結晶結構研究發現，在此類酵素活性區中，存在一個扮演類似閘道的殘基，而在 AGHO 中，其相對位置為 Tyr316。利用定點突變的方式將此位置突變成 Ala，His，Glu 和 Phe。突變株酵素具有正常的 TPQ 生成能力，但無酵素活性。以 Phe 取代的話，酵素

活性只剩 25%。Ala，His 或 Glu 等胺基酸取代，則所產生的酵素不具活性。其中影響的因素還需由進一步的實驗加以探討。

Research of Substrate Specificity of *Arthrobacter globiformis* Histamine Oxidase

Student：Jen-Gong Yang Advisor：Dr. Chiun-Jye Yuan

Department of Biological Science and Technology

National Chiao Tung University

Abstract

Copper-containing amine oxidases (CAOs) [E.C.: 1.4.3.6] are ubiquitous in nature, found in bacteria, yeasts, fungi, plants and animals. CAOs catalyze the oxidation of various primary amine substrates to their corresponding aldehydes, with the subsequent release of ammonia and hydrogen peroxide. Substrate preference depends on the enzyme source. AGHO was used as a model to study its substrate preference and kinetics to various amines to elucidate the structural characteristic of amines. The results show that the K_m value decreased in nearly linear fashion with increasing chain length of the alkyl carbon chain of amines on aromatic ring. Substrate specificity (K_{cat}/K_m) increased with increasing the hydropathy of the aromatic ring of amines.

Y316 of histamine oxidase from *Arthrobacter globiformis* has been suggested to act as a "gate" to mediate the access of substrate to TPQ. This residue has been replaced with other amino acids such as Phe, Trp, Ala, His, and Glu by site-directed mutagenesis. When Tyr316 was changed to Ala, His, or Glu, the purified recombinant proteins exhibit normal TPQ biogenesis, although their activity are not detectable. When

Tyr316 was replaced by Phe, the enzyme was active with a relative activity of around 25% compared of with that wild-type protein using histamine as substrate. These results suggest that Y316 is essential for the enzyme activity of AGHO.

Acknowledgment

兩年研究所生活一轉眼間就過去了,期間承蒙指導教授 袁俊傑老師在實驗及研究上的教導及鼓勵，以及在實驗的態度跟觀念上的指導，讓我受益良多，另外在論文寫作方面，袁老師也給予我最大的幫助，在此致上最深切的謝意；也感謝口試委員 吳東昆老師 與楊進木老師在論文上給予本人許多寶貴的建議及指教，使本論文耕趨完善。

感謝實驗室的學長姐舜評、柏文、韻舒、柏翰、雅慧、威震在生活和實驗上的不吝協助及指導，一起分享快樂和憂愁的同學昱珊、欣怡、珮玲、宗翰，學弟妹岳縉、元碩、叔青、宜芳，兩年的研究生活因為你們變的多采多姿。此外，還要感謝升耀學長，在生活和實驗上的鼓勵和照顧。

最後，特別感謝 爸爸、媽媽、政偉、雅芬、萌鈺，你們在生活上和精神上的支持和鼓勵，讓我能順利完成學業。

Contents

Table contents

Figure Contents

Appendix Contents

Abbreviation

AGAO	*Arthrobacter globiformis* phenylethylamine oxidase
AGHO	*Arthrobacter globiformis* histamine oxidase
DMAB	3-dimethylamino benzoic acid
ECAO	*Escherichia coli* amine oxidase
EDTA	[Ethylenedinitrilo]tetra acetic acid
HPAO	*Hansenula polymorpha* amine oxidase
HRP	Horseradish peroxidase
IPTG	Isopropyl- β -D-thiogalactoside
MBTH	3-methyl-2-benzothiazolinone hydrazone
NBT	Nitroblue tetrazolium
PSAO	pea seedling amine oxidase
PVDF	Polyvinylidene fluoride
SSAO	Semicarbazide sensitive amine oxidase
TPQ	2,4,5-trihydroxyphenylalanine

Introduction

Copper containing amine Oxidases (CAOs) [E.C: 1.4.3.6] constitute a family of redox active enzymes, which are present both in eukaryotes and in prokaryotes. They catalyze the two-electron oxidative deamination of primary amines into corresponding aldehydes, ammonia, and hydrogen peroxide. In prokaryotes, amine oxidases are suggested to have nutrient functions. In eukaryotes, they are involved in regulation of the concentration and physiological functions of the biogenic amines (Buffoni *et al.*, 2000; Conklin *et al.*, 2001; Jalkanen and Salmi, 2001). These enzymes are also collectively designed as SSAOs (semicarbazide-sensitive amine oxidases) due to their characteristic sensitivity Semicarbazide, a carbonyl-reactive compound, (Jalkanen *et al.*, 2001).

The CAOs are homodimers with molecular mass of 140-190kDa subunits. Each subunit contains both Cu^{2+} and a peptide-bound cofactor, 2,4,5-trihydroxyphenylalaninequinone referred to as topaquinone (TPQ). The Cu^{2+} is required for the biogenesis of TPQ in the presence of oxygen. The TPQ belongs to a unique class of quinone cofactors that derived by post-translational modifications of the side chain of tyrosine (Cai and klinman, 1994). CAOs catalyze a ping-pong type kinetic (see appendix 4) occurring in two half-reactions known as the reductive and oxidative half-reactions (Mure *et al.*, 2002), shown in Eqs. 1 and 2, respectively：

$$\boldsymbol{E}_{ox} + RCH_2NH_2 \rightarrow \boldsymbol{E}_{red} + RCHO \qquad (1)$$

$$\boldsymbol{E}_{red} + O_2 + H_2O \rightarrow \boldsymbol{E}_{ox} + H_2O_2 + NH_3 \qquad (2)$$

During the reductive half-reactions, the amine group of the substrate adds to the C-5 carbonyl group (C_5=O) of TPQ and forms an Schiff base adduct. Subsequently, the Schiff base adduct is hydrolyzed and yields the aminoquinol form of the TPQ with release of aldehydes. In the oxidative half-reactions, dioxygen is reduced, leading to the formation of hydrogen peroxide and an iminoquinone form of TPQ, from which TPQ is regenerated by hydrolysis to release ammonia. The mutagenesis studies of ECAO showed that Asp383 may be the active base playing roles in assisting substrate binding to TPQ and abstracting the C-H proton from substrate during catalysis (Wilmot, *et al.,* 1997).

It has been demonstrated that TPQ is derived from a specific tyrosyl residue in the highly conserved Asn-**Tyr**-(Asp/Glu)-Tyr sequence by self-processed oxidation in the presence of copper ion and molecular oxygen. Copper ion is crucial for TPQ formation and is unreplacable with other metal ions, such as zinc, cobalt, and nickel (Cai *et al*. 1997; Kishishita *et al.* 2004). From the spectroscopic investigations, CAOs show a characteristic broad absorption band with a λ_{max} at around 480 nm, arising from the oxidized form of TPQ. Depending on the source of CAOs, the λ_{max} can vary from 472 to 500 nm (Mure *et. al*., 2002).

Recent X-ray crystallographic studies of the enzyme from *Arthrobacter globiformis* phenylethylamine oxidase (AGAO) (Kim *et al.*, 2002) had shown that TPQ biogenesis may follow five intermediate steps (see appendix 3). At first, copper binds anaerobically to the enzyme by coordinating with the imidazole groups of three histidines and two water molecules, providing an approximately square-pyramidal geometry. Following the binding of dioxygen at a site near the precursor tyrosine, the first oxygenation at the C3 position on the aromatic ring of Tyr (corresponding to C5 of TPQ) occurs and forms DPQ (dopaquinone). The quinone ring of DPQ then rotates around the C^{β}-C^{γ} bond by ~180° for the second modification (or oxidation) at the C2 position of the aromatic ring. Other important finding from the structural study is that the imidazole ring of one of the tree Cu-binding histidine residues, His592, can adopt two distinct conformations in both apo-AGAO and holo-AGAO crystal structures. The mutation of the H592 to Ala (H592A) delays the formation of TPQ. The exogenous imidazole could markedly promote the formation of TPQ, in H592A mutant, although the process is show mutant possesses very low catalytic activity (Matsunami *et al.*, 2004).

The X-ray crystallographic structures of CAOs from *Escherichia coli* (ECAO), pea seedling (PSAO), *Hansenula polymorpha* (HPAO), and *Arthrobacter globiformis* (AGAO) has been solved (Parsons *et al.,* 1995, Kumar *et al.,* 1996, and Li *et al.,* 1997, and Matthew *et al.,* 1997). The results show that all four CAOs share similar polypeptide folds and 3D structure, although their sequence identities are low (Wilce M. C. J. *et al.,* 1997). Each subunit of a dimer is composed of three domains, and a conspicuous β-ribbon arm extending from it. The extending β-ribbon arm then embraces the other subunit to hold the dimer structure. In the active form of holo-AGAO, the Cu^{2+} ion is still coordinated by three histidine residues and two water molecules, it may not play any role in the catalysis of cycle. The TPQ in amine oxidases is highly flexible, as indicated, by the crystal structures of holo-AGAO and other amine oxidases (Matthew *et al.,* 1997).

CAOs exhibit broad substrate specificities, depending on the enzyme sources. The substrates specificities of mammalian CAOs are broad, either aromatic or aliphatic amines can be substrates. While plants CAOs show preference to diamines, such as putrescine and cadaverine. These enzymes show certain activity also toward some mono- and polyamines (Paolo *et al.*, 1995). Bacterial CAOs oxidize aromatic amines such as histamine, dopamine, phenylethylamine, and tyramine most efficiently (Eiichi *et al.*, 1994). The reason why CAOs from different sources exhibit different substrate specificities is still unknown. Semicarbazide-sensitive amine oxidases (SSAO) in the mammalian tissues are capable of deaminating both aliphatic amines, including methylamine, allylamine, aminoacetone (Deng and Yu, 1999), and aromatic amines, including tyramine, dopamine, and histamine. Recent work suggests that elevated serum SSAO activity may cause injury of endothelial. Formation of cytotoxic metabolites (e.g., formaldehyde) and increasing oxidative stress lead to initiation or progression of atherosclerosis (Magyar *et al*., 2001; Karádi *et al*., 2002).

The exact physiological role of the mammalian SSAOs is presently not well understood. SSAO catalyzes the amino-transferase type reaction producing aldehydes, ammonia, and hydrogen peroxide. In mammalian, these products are potentially cytotoxic and may be involved in the pathogenesis of atherosclerosis and diabetic vascular complications. There are several pathological states, such as diabetes mellitus, congestive heart failure, multiple types of cerebral infarction, uremia, and hepatic cirrhosis exhibit increased serum SSAO activity, (Magyar *et al*., 2001). The elevation of amine level in the ciculation might be responsible for the induction of SSAOs activity. Several inhibitors for mammalian CAOs are well studied. These mammalian enzymes can be completely and irreversibly inactivated by the derivatives of hydrazine, such as phenelzine, isonialzid, trancyproamine, and 2-hydrazinopyridine (2-HP). The crystal structure of 2HP-inhibited ECAO shows that the 2-HP binds covalently at the O5 position of TPQ, mimicing the Schiff base complex of substrate and enzyme (Saysell *et al*., 2002). Phenylhydrazine (PHZ) was used to identify the TPQ cofactor due to the formation of the intense visible adduct between TPQ and PHZ (De *et al*., 1996). This intensely yellow-coloured adduct with an adsorption maximum at 438 nm (Choi *et al.*, 1995) provides an important tool to identify the formation of TPQ cofactor in CAOs. Substrate-like inhibitors have been used in the biochemical and kinetic studies of amine oxidases (Shepard *et al*. 2002). A well-designed substrate-like inhibitor, may help to clarify the differences in substrate specificities among CAOs and can be used as a lead for further drug design.

The *Arthrobacter globiformis* histamine oxidase was identified (Shimizu *et al.*, 1994). The *Coryneform* bacterium *A. globiformis* produces two copper amine oxidases, phenylethylamine oxidase and histamine oxidase, when induced by phenylethylamine and histamine, respectively (Choi *et al.*, 1995). The sequence homology between these two enzymes is about 61%. A channel-like active site structure has been found in the AGAO structure (Matsuzaki and Tanizawa, 1998). The internal surface of the channel leading to TPQ becomes more hydrophobic as evidenced by the presence of Trp, Leu, and Phe residues. The side chain of Tyr296 at the end of the channel probably acts like a "gate" for the access of substrates to the TPQ, and is conserved in many amine oxidases (Chang, 2003) (see appendix 6).

We have subcloned the gene of *A. globiformis* histamine oxidase. The histamine oxidase have been overproduced and purified as a fusion protein with a $(His)_6$-tag (Lin, 2002). Previous work from laboratory has shown that the optimal pH of AGHO was 6.5 to 7.5, using buffers over the range of pH 5.0 to 11.0. The thermal stability of AGHO is about 25℃ to 30℃ (Chang, 2003). We also generated a set of Tyr316 (corresponding to Tyr296 in AGAO) mutants of AGHO, termed Y316A, Y316E, Y316F, and Y316H to investigate the effect of mutation to the TPQ biogenesis, pH profile, and thermal stability. In this thesis, evidence is presented to show that mutation at Y316 may influence the enzyme activity. In this present study we report on the kinetics studies of AGHO with various aromatic amine analogues and some aliphatic amines.

Materials and Methods

1. Materials

Horseradish peroxidase (HRP), DMAB (3-dimethylaminobenzoic acid), MBTH (3-methyl-2-benzothiazolinone hydrazone hydrochloride), and amines (see the Appendix 1)were purchased from Sigma except that 2,3-Dihroxyphenylethylamine-HBr and 2,4-Dihroxyphenylethylamine-HCl 1/4 Hydrate were kindly gift of Dr. Brady, L. S. and Dr. Tanga, M. J. of National Institute of Mental health, NIH, Bethesda, MD, USA. Bradford reagent was obtained from Bio-Rad. Immobilon ^{TM} –P transfer membrane was from Millipore.

2. Methods

2.1 Construction of expression plasmid

The Y316A, Y316H, Y316W mutants of AGHO in pUC-T and the expression vector pET30(-S)/AGHO were constructed previously in our laboratory (Lin, 2002; Chang, 2003). The AgeI and BsaI fragments of Y316 mutants of AGHO gene (959 bp) were purified from agarose gel and recovered using Gel/ PCR DNA Fragments Extraction Kit (GENEAID). The purified DNA fragment were then used to replaced the AgeI/BsaI fragment of AGHO gene in pET30(-S)/AGHO.

2.2 Site-directed mutagenesis

Y316E and Y316F mutants of AGHO were generated using QuickChange™ Site-Directed Mutagenesis protocol (STRATAGENE) with pUT-T/AGHO-I as a template (Lin Y. H., 2002). The reaction reagent contained 50 ng DNA template, 1 μM forward and reverse primers, 2.5 U *Puf*Turbo DNA polymerase, and 0.5 mM dNTP in a final volume of 50 μL. The PCR condition was set following the protocol of manufacturer. Add 10 U Dpn I restriction enzyme into the resulting PCR product to remove the original methylated template. The reaction was performed by incubating at 37 ℃ overnight. The Dpn I-treated PCR product (10 μL) was then transformed into DH5α competent cells and screened for mutants. The mutations of AGHO were confirmed by DNA sequencing.

2.3 DNA sequencing

The DNA sequencing was performed on the ABI 377 autoseqencer using Big Dye DNA sequencing kit (ABI). The reaction buffer contained 200-500 ng DNA template, 0.67 μM sequencing primer, 3 μL Big Dye DNA sequencing kit (ABI) in a final volume of 15 μL. The PCR condition was set as directed by manufacturer. Briefly, the PCR reaction mixture was first heated at 96 ℃ for 5 min, followed by running thermal cycles 25 cycles DNA denaturing of following at 96 ℃ for 10 sec for, the DNA-primer annealing at 50 ℃ for 5 sec, and DNA extension at 60 ℃ for 4 min. The final DNA extension was performed at 60 ℃ for 10 min. The resulting PCR product can be used directly or stored at 4 ℃. To 15 μL final PCR mixtures, 68 μL 95% ethanol was added to precipitate fluorescent-labeled sequencing products. The PCR product mixture and ethanol were mixed well in a 1.5 mL microfuge tube and kept at -20 ℃ for at least 1 h. The resulting solution was centrifuged at 14,000×g for 60 min to precipitate the nucleic acids. The pellet was then washed 2-3tines with 75% ethanol. Remove the supernatant carefully and air-dry the DNA pellet. The fluorescent dye labeled DNA pellet was then dissolved in 4 μL sequencing gel loading dye with pipetting and subjected to DNA sequencing. The sequence data was obtained by ABI Prism™ 377 DNA autosequencer.

2.4 *E coli* expression and purification of AGHO

The recombinant AGHO was overproduced in *E. coli* BL21 (DE3) cells carrying plasmid pET30b (-S)/AGHO. Cells were grown at 37 ℃ in 200 mL LB medium supplemented with 25 μg/mL kanamycin and cultivated until the cell density reached A_{600nm} =0.4~0.6. Stock isopropyl-1-thio-**β**-D-galactopyranoside (IPTG) was added to give the final concentration of 50 μM. The bacteria were then further cultivated at 25 ℃ for 8 h in the presence or absence of 50 μM $CuSO_4$. The cells then were harvested by centrifugation at 6,000×g for 10 min.

The cell pellet was resuspended in 5 volumes of buffer A (50 mM potassium phosphate buffer, pH 6.8 containing 50 μM $CuSO_4$) or buffer B (50 mM potassium phosphate buffer, pH 6.8 containing 1 mM EDTA).

The cell suspension was then disrupted on ice by ultrasonic disintegration with the instrument setting of sonic dismembrator (550, Fisher Scientific). The resulting lysate was centrifuged at 14,000×g for 10 min to remove insoluble particulates. The supernatant was first fractionated with ammonium sulfate (0-50%). The precipitate of 50% (w/w) ammonium sulfate was dissolved in 1 mL buffer A or buffer B and dialyzed against the same buffer for 24 h. The buffer was renewed every 8 h. To remove most of EDTA, the enzyme solution dialyzed against buffer B would be transferred to 50 mM potassium phosphate buffer (pH 6.8) during the last buffer change.

The enzyme solution was then applied to a 1 mL HiTrap-chelating column (Amersham Biosciences). The column was prepared following manufacturer's protocol. Briefly, the column was washed with 5 mL distilled water prior to loading 1 mL charge buffer (100 mM $NiSO_4$) to charging the column. Wash column with 1 bed volume distilled water to remove the unbound metal ions. After column preparation, the column was equilibrated with 5 bed volumes of binding buffer (20 mM Tris-HCl, pH 7.9, 500 mM NaCl, 5 mM imidazole) Samples were centrifuged at 10,000×g for 15 min prior to loading on the column. Wash the column with 10 bed volumes of binding buffer. To further remove non-specifically bound proteins the column can be a washed with binding buffer containing 60 mM imidazole. Protein was eluted with binding buffer containing 500 mM imidazole. If necessary, the eluted protein can be dialyzed overnight against 50 mM potassium phosphate buffer, pH 6.8.

2.5 Protein concentration determination

Protein concentration was determined by Bradford protein assay (Bio-Rad) using bovine serum albumin as a standard.

2.6 Activity Assay

Amine oxidase activity was measured spectrophotometrically by monitoring H_2O_2 production through a coupling assay by horseradish peroxidase (HRP) using DMAB (3-dimethyl-aminobenzoic acid) and MBTH (3-methyl-2-benzothiazolinone hydrazone) as substrates (Stoner, 1985). A DMAB-MBTH conjugated purple indamine dye formed during reaction can be measured at absorbance of 595 nm. Assays were carried out in a reaction buffer containing 50 mM sodium phosphate buffer, pH 7.4, 2 μg enzyme and 100 μM amine substrate in a total volume of 0.5 mL at 30 ℃ for 30 sec or longer. The detection buffer contains 2.5 U horseradish peroxidase, 2 mM DMAB, 0.04 mM MBTH in a final volume of 0.5 mL. Blank assay medium did not contain substrates. The Cu^{2+}-deficient inactive enzyme was incubated at 30 ℃ for 30 min with 50 mM $CuSO_4$ in 50 mM sodium phosphate buffer (pH 6.8), before subjecting activity assay. The enzymatic reaction was started by mixing substrate and AGHO in a reaction buffer at room temperature for 30 sec. The reaction was stopped by adding 0.5 mL detection buffer, mix well and measure the colored product at absorption of 595 nm. Absorbance measurement were obtained with a

Hitachi U-3010 at 30 ℃ using quartz cuvettes with 1 cm path length.

2.7 H_2O_2 Standard Curve

The procedure is the same as that of activity assay except that amine oxidase and substrates were replaced with H_2O_2 in amounts from 1.0 to 20 nmoles. The standard curve of H_2O_2 concentration and O.D. was illustrated in Fig. 1.

2.8 Kinetic Measurement

Substrate stock solutions were freshly prepared in distilled water or methanol. The concentration of substrate in the kinetic study varies based on type of substrate due to substrate inhibition effect. The reaction time was 30 sec for most of amine substrates except benzylamine, phenylpropylamine, tryptamine, and D, L-octopamine. The oxidation of substrates was determination by coupled assay (as described in Activity Assay). The data were fitted non-linearly by at least six or more substrate concentrations. The curve fitting was performed using Michaelis-Menten equation on the SIGMA plot program Enzyme Kinetics Module 1.1. Those substrates demonstrating substrate inhibition were also using Eq. 3:

$$V = Vmax / (1 + Km/[S] + [S]/Ki) \quad (3)$$

2.9 Electrophoresis and Redox-Cycling Staining

All SDS PAGE was performed with a Bio-Rad Mini Protein II apparatus. 10% polyacryamide gels were prepared. Enzyme samples were boiled for 5 min in the presence of 5% 2-mercaptoethanol before loading onto the SDS-polyacryamide gel. After electrophoresis, the gel was stained with Coomassie Blue. Standard proteins for calibration (kDa) were MBI marker #SM0431.

For redox-cycling staining, proteins separated by 10% SDS-polyacryamide gels were electroblotted on to a 0.45 μm nitrocellulose membrane in an ice-cold transfer buffer (25 mM Tris, pH 8.3, 192 mM Glycine, 20% (v/v) methanol) at a constant current of 200 mA for 2 h. The nitrocellulose membrane was then immersed in the Glycinate/NBT solution (0.24 mM Nitro Blue Tetratzolium in 0.1 M potassium glycine , pH 10) at 25 ℃ for 30-45 min in the dark. The quinoproteins would be stained as blue-purple bands on the membrane.

2.10 Phenylhydrazine Titrations

Reactive TPQ in AGHO or its mutants can be quantified by the titration with phenylhydrazine, which forms a stable, intensely yellow-coloured adduct with a maximum absorption at $\lambda \approx 438$ nm (Choi *et al.*, 1995). The phenylhydrazine stock solution (1 mM) was prepared fresh by dissolving phenylhydrazine hydrochloride in distilled water and storing it at 4 ℃ in the dark before using. TPQ titration of

AGHO was carried out by step-wise adding phenylhydrazine stock solution in 1 ml of enzyme (12.5 μM) to the final concentrations of 0, 1.0, 2.0, 4.0, 6.0, 10.0, 12.0, 13.0, 15.0, and 17.0 μM. Each spectrum was recorded 15 min after incubation at 30 ℃ following each addition.

Results

Expression and Purification of Wild-type and Mutant Histamine Oxidases— The production of an active quinone-containing form of CAOs is dependent on the presence of Cu^{2+} ions. We prepare both the Cu^{2+}-deficient inactive precursor of AGHO and the Cu^{2+}-containing active enzyme. The purified AGHO (Cu^{2+}-containing active form) exhibited a brownish pink color, whereas the Cu^{2+}-free form inactive enzyme was colorless. Although the enzyme activity under two different expression conditions (see Methods 2.4) seems different, the purification efficiency is the same (Table.3). The Y316A, Y316E, Y316F, and Y316H mutants were also purified as a copper/TPQ-free, inactive form to homogeneity as indicated by SDS-polyacryamide gel electrophoresis (Fig. 2).

Titration with Phenylhydrazine— The presence of a quinone moiety in the *A. globiformis* histamine oxidase was investigated by reaction with phenylhydrazine (Paz *et al*., 1991). The TPQ biogenesis in the Cu^{2+}-reconstituted enzyme was titrated with the carbonyl reagent phenylhydrazine, which reacts with the topaquinone to form a yellow adduct. The enzyme solution was incubated with phenylhydrazine at 30 ℃ for 15 min, the full spectrum of the enzyme was scanned and recorded. The TPQ in AGHO was titrated with 0~17 μmole phenylhydrazine. An absorption peak at λ_{max}= 438 nm increased with increasing the concentration of phenylhydrazine (Fig. 3A). The endpoint of titration was approximated at about ~ 12 nmole (Fig. 3B).

Upon calculation, the ratio of TPQ: AGHO monomer is about 0.5:1.0.

Relative Activity of AGHO with Various Substrates—Although histamine was reported to be the primary substrate for AGHO, other amines were also indicated to be catalyzed by this enzyme (Shimizu, 1994). To confirm this observation, the reactivity of Cu^{2+}-reconstituted active AGHO to various, natural or Xenobiotic amines (Appendix. 1) were treated. The relative activities (compared with histamine) of other amines at 0.1 mM are listed in table 3. Accordingly, AGHO exhibited higher reactivity to phenylethylamine (154%), tyramine (107%) dopamine (125%) than to the histamine. AGHO exhibited moderate activity to some amines, including 2,3-dihydroxypenylethylamine (84%), 2,4-dihydroxypenylethylamine
(80%), 3-methoxyphtnylethylamine (67%) and 4-methoxy-phenylethylamine (55%). AGHO showed a little or no activity to benzylamine (0.5%), serotonin (12%), Norepinephrine (4%), and all the aliphatic amines studied (Table. 3). Notably, all amines except histamine exhibit strong to moderate inhibition at higher concentration.

Kinetic studies of AGHO with Histamine and its derivative—Although CAOs exhibit common mechanistic features, the substrate specificities of these enzymes appear to be different. The amine oxidases from bacteria show a preference for aromatic amines. In this work, we tend to investigate the structural characteristics of various amines that may influence their binding affinity to AGHO. Tables 4-6 show the kinetic constants (K_m, K_{cat}, K_{cat}/K_m) of AGHO to various structurally related amines. Initial rates of AGHO at each concentration of corresponding amine substrate were determined at 30 ℃, pH 7.0 for 0-10 min. The non-linear curve of initial rate vs. substrate concentration was fitted to the appropriate Michaelis-Menten equation or to Eq. 3. The plots of initial rate vs. substrate concentration for various amines were shown in Fig. 4-9. The results show that almost all amines (except histamine) exhibit strong to moderate substrate inhibition to recombinant AGHO. The substrate inhibition effect was not significant in histamine oxidation. As shown in Table 5, AGHO exhibited slightly increasing K_m values with increasing hydroxyl groups on the aromatic ring of the phenylethylamine derivatives. Recombinant AGHO shows a preference to more hydrophibic amines, as indicated by the K_{cat}/K_m, a specificity constant, for phenylethylamine (1.11), tyramine (0.77), 2,3-Dihydroxy-phenylethylamine (0.54), 2,4-Dihydroxyphenylethylamine (0.53), and 3,4-dihydroxyphenylethylamine (0.42)(Table 5). The result suggests that K_{cat}/K_m decrease with decreasing hydropathy. The K_m for histamine was about twenty seven times higher than that of tryptamine.

Next, we want to study the effect of different chain length connecting amine group and aromatic ring to catalytic activity of AGHO. Benzylamine, phenylethylamine, phenylpropylamine, and phenylbutylamine were chosen in this study (Table 6). As shown Table 6, $\boldsymbol{K_M}$ values of amines decrease in nearly linear fashion with increasing chain length of the alkyl carbon chain connecting amine and aromatic groups. The catalysis of AGHO for benzylamine and phenylpropylamine was slower. However, the K_{cat} decrease drastically with increasing the alkyl chain length. This postulation was confirmed by the kinetic studies of 2 more hydrophobic methoxyl derivatives of phenylethylamine, 3-methoxy-phenylethylamine (K_m=15.97 ± 1.76,

K_{cat}=16.67 ± 0.99, K_{cat}/K_m=1.04) and 4-methoxy-phenylethylamine (K_m=16.73 ± 3.63, K_{cat}=17.60 ± 2.20, K_{cat}/K_m=1.05). The decreasing substrate preference was with increasing hydroxyl group numbers on the benzene ring of the aromatic amines, indicating the binding affinity is suppressed with the increasing the hydrophilicity of aromatic amines. However, the effects of methoxyl group substituted in the *para* and *inter* position increase their inhibitory potency as indicated by e K_i values for 3-methoxy-phenylethylamine and 4-methoxy-phenylethylamine, were 56.69 ± 5.74 μM, and 32.18 ± 5.90 μM, respectively. The oxidation rate of aliphatic amine were too slow to determinate the kinetic parameters.

Catalytic properties of Cu^{2+}-reconstituted enzymes—Y316, at in the end of the substrate channel, is considered as a "gate" for substrates to access TPQ. It is hypothesized that it may play a key role in mediating the substrate specificity of many CAOs. All five Y316 mutants can be purified as wild type AGHO dose; however, mutations at Y316 alter amine oxidase activity (Table. 2). After incubation with 50 μM $CuSO_4$ at 30 ℃ for 30 min, three Y316 AGHO mutants, Y316A, Y316E, and Y316H, showed no catalytic activity toward aromatic amines, including histamine, phenylethylamine, or tyramine, as well as aliphatic amines, including methylamine or ethylamine. The specific activity of AGHO Y316F decreased 75%, compared with that wild-type enzyme in the presence of 0.1 mM histamine. Interestingly, the TPQ biogenesis of all AGHO Y316 mutants were not altered as illustrated in Fig. 10 and Fig. 11.

In vitro reconstitution with 1 mM copper did not influence the specific activity of Cu^{2+}-reconsituted wild-type enzyme. Even the enzyme was incubated with 50 μM $CuSO_4$ at 4 ℃ for 24 hr, the activity of enzyme did not increase. The wild-type and Y316 mutants could be completely reconstituted to active enzyme when incubation with 50 μM $CuSO_4$ at 30 ℃ for 30 min.

Discussion

In this study, we have demonstrated that the oxidative modification of the precursor tyrosine to TPQ could be completed in the presence of 50 μM $CuSO_4$. According to the result of redox-cycling staining, wild type AGHO was active as a result of the formation of TPQ by a self-processing mechanism. The storage time of the apo-form AGHO at 4 ℃ was longer then Cu^{2+}-containing active form AGHO. This is probably because Cu^{2+} can induce a oxidative damage on the enzyme due to its strong oxidative catalytic activity.

The correlations between specific activity and titratable TPQ have been described by Klinman and co-workers (Janes *et al.,* 1991; Cai *et al.,* 1994). It is presently unclear whether low TPQ to CAO ratio (normally around 0.6) is due to low TPQ-to-copper ratios reflect incomplete organic cofactor biogenesis or due to the conformations of the matured enzymes in which the quinone cofactor is inaccessible to phenylhydrazine.

It has long been recognized that CAOs generally oxidize a variety of primary amines. For example, AGAO oxidizes a range of aromatic, alkyl, and aliphatic primary amines. In the case of PSAO, the preferred substrates are primary diamines, such as putrescine and cadaverine. The HPAO preferentially catalyzes oxidation of the aliphatic amines, such as methylamine and ethylamine.

In this work, we showed that AGHO prefer hydrophobic amines as its substrates. The K_{cat}/K_m values of hydrophilic amines, including dopamine or 3,4-dihydroxyphenylethylamine (K_{cat}/K_m=0.42), tyramine or 3-hydroxyphenylethylamine (K_{cat}/K_m=0.77), 2,3-dihydroxy-phenylethylamine (K_{cat}/K_m=0.54), and 2,4-dihydroxyphenylethylamine (K_{cat}/K_m=0.53), were lower than that of hydrophobic amines, such as phenylethylamine (K_{cat}/K_m=1.11), 3-methoxyphenylethylamine (K_{cat}/K_m=1.04), and 4-methoxypheylethylamine (K_{cat}/K_m=1.05). Substitution has a modest effect on K_{cat}. The hydrophobicity is probably the determinant in substrate to affect its binding to AGHO, implying the presence of a lipophilic binding pocket at the active site of AGHO (Wilce *et al.*, 1997). The relationship between the hydropathy and the K_{cat}/K_m value of amine were demonstrated in this study. Although the hydropathy of the amines studied in this work is unknown, the scold of corresponding amino acids of these amines, such as histamine, phenylethylamine, tyramine, and tryptamine, may provide a reference about the hydropathy of the amines (Plaecz, 2002). From the analysis of lipophilicity scales, phenylalanine (with a scold of 179) is more hydrophobic than that of Trp (147), Tyr (64), and His (-34). The K_{cat}/K_m value of those amines follows the same fashion to the hydropathy of the corresponding amino acids. This result indicates that hydrophobicity of the amines is one of the essential factors that mediate the binding and recognition of amines by the AGHO.

The substrate specificity of CAOs is the challenging topic. Since amine substrates are recognized in their protonated, positively charged form, the electrostatic potential and surface topology at the entrance to the channel may be important for substrate recognition. In the previous inhibition study (Shepard *et al.*, 2002), 1,4-diamino-2-chloro-2-butene and 1,6-diamino-2,4-hexadiyne effectively inhibit six amine oxidases (AGAO, ECAO, PPLO, PSAO, BPAO, and EPAO). Distinctions among the active sites must be responsible for differentiating the chemical interactions between the inhibitors and enzymes. With the crystal structures of amine oxidases from different source, structure-like substrate or inhibitor study might be combined with bioinformatics tool for the study of substrate specificity.

Based on the clinical investigation, the determination of SSAO activity in mammalian might be a candidate biochemical marker for screening healthy people with high risk of atherosclerosis for the presence of early atherosclerotic lesions. The amine content of fish can food is the determination of fresh order. The clarification of substrate specificity among different amine oxidases is helpful for biosensor application and medical drug design.

AGHO shows a clear substrate preference for aromatic amines. It is also apparent that substrate specificity of AGHO depends on the hydrophobicity of amines and the length of alkyl amine on the aromatic ring.

Phenylethylamine is a good substrate for AGHO. Two derivatives, benzylamine and phenylpropylamine, also contain a benzene ring but with different length of alkyl amine group are poor substrates for AGHO. AGHO shows a slow catalytic activity to benzylamine in our assay conditions. The aliphatic amine, such as methylamine or ethylamine, also have slow reaction rate. Structural comparison of benzylamine, phenylethylamine, methylamine, and ethylamine revealed that the main differences were phenolic ring. It is reasonable to assume that there was existence of a cavity of active site holding aromatic ring of amines for catalytic reaction. The appropriate chain length of alkyl carbon chain determines good substrate or not.

The amino acid sequence alignment (Appendix. 7) shows that the residues acted as “gate” were Phe298 in PSAO, Tyr381 in ECAO, Tyr296 in AGAO, Ala317 in HPAO, and Y316 in AGHO. In the structure of native ECAO, the active site is buried with no obvious entry route for the monoamine substrates. In the crystal structure of ECAO complex with 2-HP (Wilmot *et al.*, 1997), the pyridine ring of 2-HP is almost completely buried and has displaced Tyr381, which forms a π/π ring-stacking interaction with the pyridine ring. All these differences could contribute to the molecular basis for substrate specificity among these enzymes. We show that the role of Y316 could influence the reaction of enzyme and substrates. The Y316 mutant enzymes purified to homogeneity in the apo forms, and could be also activated at excess Cu ions. The activity assay of Y316 mutant enzymes show that the Y316 could act like a “gate” but was not responsible for substrate specificity. The replacement of a bulky functional residue, tyrosine, by a nonfunctional or positive charge group, such as alanine, histamine, and glutamine, need more investigation to clarify how it cause the loss of activity.

In conclusion, we have shown here that the mutation of Y316 residue influence the catalytic activity. In this studies, the substrate specificity of Cu_{2+}-reconstituted active recombinant AGHO have revealed that hydrophobicity is one of the essential factors that determined the affinity of AGHO to its substrates.

Reference

Bollag, D. M., Rozycki, M. D., and Edelstein S. J. (1996) Ammonium sulfate precipitation (salt out). In *Protein Methods* (2nd ed.), 91-93 and 394-395.

Buffoni F. and Ignesti G. (2000) The Copper-Containing Amine Oxidases: Biochemical Aspects and Functional Role, *Mol. Genet. Metab.* 71, 559-564.

Cai, D. and Klinman, J.P. (1994) Evidence of a self-catalytic mechanism of 2,4,5-trihydroxyphenylalanine quinone biogenesis in yeast copper amine oxidase. *J. Biol. Chem.* 269, 32039-32042.

Cai, D., Williams, N. K., and Klinman J. P. (1997) Effect of metal on 2,4,5-tridroxyphenylalanine (topa) quinone biogenesis in the *Hansenula polymorpha* copper amine oxidase. *J. Biol. Chem.* 272, 19277-19281.

Chang S. P. (2003) Characterization of *Arthrobacter globiformis* histamine oxidase by mutagenesis. A thesis submitted to institute of Biological Science and Technology National Chiao Tung University In partial Fulfillment of the requirements for the Degree of Master of Science in Biological Science and Technology.

Choi, Y. H., Matsuzaki, R., Fukui, T., Shimizu, E., Yorifuji, T., Sato, H., Ozaki, Y. and Tanizawa, K. (1995) Copper/topa quinone-containing histamine oxidase from *Arthrobacter globiformis*. Molecular cloning and sequencing, overproduction of precursor enzyme, and generation of topa quinone cofactor. *J. Biol. Chem.* 270, 4712-4720.

Choi, Y. H., Matsuzaki, R., Suzuki, S., and Tanizawa, K. (1996) Role of conserved Asn-Tyr-Asp-Tyr sequence in bacterial copper/ 2,4,5-trihydroxyphen-ylalanyl quinone-containing histamine oxidase**.** *J. Biol. Chem.* 271, 22598–22603.

Conklin D. J., Boyce C. L., Trent M. B., and Boor P. J. (2001) Amine metabolism: a novel path to coronary artery vasospasm. *Toxicol. Appl. Pharmacol.* 175, 149-159.

De Biase D., Agostinelli E., de Matteis G., Mondovi B., and Morpurgo L. (1996) Half of the sites reactivity of bovine serum amine oxidase: reactivity and chemical identity of the second site. *Eur. J. Biochem.* 237, 93-99.

Deng Y. and Yu P. H. (1999) assessment of the deamination of aminoacetone, an endogenous substrate for Semicarbazide-sensitive amine oxidase. *Anal. Biochem.* 207. 97-102.

Eiichi, S., Keiichi, O., Shigeo, T., Yuzuru, K., Katsuyuki, T. and Takamitsu, Y. (1997) Purification and properties of phenylethylamine oxidase of *Arthrobacter globiformis*. *Biosci. Biotech. Biochem*. 61(3), 501-505.

Eiichi, S., Takuya, O., Katsuyuki, T. and Takamitsu, Y. (1994) Histamine oxidase, a Cu^{2+}-quinoprotein enzyme of *Arthrobacter globiformis*. *Biosci. Biotech. Biochem.* 58(11), 2118-2120.

Fluckiger, R., Paz, M.A., Henson, E., and Gallop, P. M. (1993) Glycine-dependent redox cycling and other methods for PQQ and quinoprotein detection, 331-341. In Davidson V. L. (ed.), *Principles and applications of quinoproteins* Marcel Dekker, New

York.

Frebort I. and Adachi O. (1995(a)) Copper/ Quinone- Containing Amine Oxidase, an Exciting Class of Ubiquitous Enzymes, *Journal of Fermentation and Bioengineering*, 80, 625-632.

Iwaki S, Ogasawara M, Kurita R, Niwa O, Tanizawa K, Ohashi Y, and Maeyama K. (2002) Real-time monitoring of histamine released from rat basophilic leukemia (RBL-2H3) cells with a histamine microsensor using recombinant histamine oxidase, *Anal. Biochem.*, 304, 236-43.

Jalkanen, S. and Salmi M. (2001) Cell surface monoamine oxidases: enzymes in search of a function. *EMBO J.* 20, 3893-3901.

Janes, S. M. and Klinman, J. P. (1991) An investigation of bovine serum amine oxidase active site stoichiometry: evidence for an aminotransferase mechanism involving two carbonyl cofactor per enzyme dimer. *Biochemistry* 30, 4599-4605.

Karádi I., Mészáros Z., Csányi A., Szombathy T., Hosszúfalusi N., Romics L., and Magyar K. (2002) Serum Semicarbazide-sensitive amine oxidase (SSAO) activity is an independent marker of carotid atherosclerosis. *Clinica Chimica Acta* 323, 2002.

Kim M., Okajima T., Kishishita S.,Yoshimura M., Kawamori A., Tanizawa K., and Yamaguchi H. (2002) X-ray Snspshots of Quinone Cofactor Biogenesis In Bacterial Copper Amine Oxidase, *Nat. Struct. Biol.* 9,591-596.

Kishishita S., Okajima, T.,Kim, M., Yamaguchi, H., Hirota, S., Suzuki, S., Kuroda, S., Tanizawa, K., and Mure, M. (2003) Role of copper ion in bacterial copper amine oxidase: spectroscopic and crystallographic studies of metal-substituted enzymes. *J. Am. Chem. Soc.* 125, 1041-1055.

Kuchar, J. A. and Dooley, D. M. (2001) Cloning, sequence analysis, and characterization of the Lysyl oxidase from *Pichia Pastoris*. *Journal of Inorganic Biochemistry* 83, 193-204.

Lin Y. H. (2002) Expression, mutagenesis and characterization of *Arthrobacter globiformis* amine oxidase I (histamine oxidase). A thesis submitted to institute of Biological Science and Technology National Chiao Tung University In partial Fulfillment of the requirements for the Degree of Master of Science in Biological Science and Technology.

Lu P. Y. (2000) The development of a rapid assay system for biogenic amines. A thesis submitted to institute of Biological Science and Technology National Chiao Tung University In partial Fulfillment of the requirements for the Degree of Master of Science in Biological Science and Technology.

Magyar, K., Meszaros, Z., and Matyus, P. (2001) Semicarbazide-sensitive amine oxidase. Its physiological significance. 73, 1393-1400.

Matsunami, H., Okajima, T., Hirota, S., Yamaguchi, H., Hori, H., Kuroda S., and Tanizawa, K. (2004) Chemical rescue of a site-specific mutant copper amine oxidase for generation of the topa quinone cofactor. *Biochemistry* 43, 2178-2187.

Matsuzaki R. and Tanizawa K. (1998) Exploring a Channel to the Active Site of Copper/Topaquinone-Containing Phenylethylamine Oxidase by Chemical Modification and Site-Specific Mutagenesis, *biochemistry* 37, 13947-13957.

Miller J. R., and Edmondson D. E., (1999) Structure-activity relationship in the oxidation of para-substituted benzylamine analogues by recombinant human liver monoamine oxidase A, *Biochemistry* 38, 136670-13683.

Mure, M., Mill, S. A., and Klinman J. P. (2002) Catalytic mechanism of topa quinone containing copper amine oxidase. *Biochemistry* 41 (30), 9269-9278.

Murray, J. M., Kurtis, C. R.; Tambyrajah, W., Saysell, C. G., Wilmot, C. M., Parsons, M. R., Phillips, S. E. V., Knowles, P. F., McPherson, M. J. (2001) Conserved Tyrosine-369 in the Active Site of *Escherichia coli* Copper Amine Oxidase Is Not Essential. *Biochemistry* 40(43), 12808-12818.

Palecz B., (2002) Enthalpic Homogeneous Pair Interaction Coefficients of L-r-Amino Acids as a Hydrophobicity Parameter of Amino Acid Side Chains. *J. Am. Chem. Soc.* 124, 6003-6008.

Paolo, M. L. D., Vianello F., Stevanato R., and Rigo A. (1995) Kinetic characterization of soybean seedling amine oxidase. *Arch. Biochem. Biophys.* 323, 329-334.

Paz, A. M., Fluckiger R., Boak A., Kagan H. M., and Gallop P. M. (1991) Specific detection of quinoproteins by redox-cycling staining. *J. Biol. Chem.* 266, 689-692.

Prabhakar, R. and Siegbahn, P. E. M. (2004) A theoretical study of the mechanism for the biogenesis of cofactor topaquinone in copper amine oxidases. *J. Am. Chem. Soc.* 126, 3996-4006.

Saysell C. G., Tambyrajah W. S., Murray J. M., Wilmot C. M., Phillips S.

E. V., McPherson M. J., and Knowles P. F. (2002) Probing the catalytic mechanism of *Escherichia coli* amine oxidase using mutational variants and a reversible inhibitor as a substrate analogue. *Biochem. J.* 365, 809-816.

Shepard, E. M., Smith, J., Elmore B. O., Kuchar, J. A., Sayre L. M., and Dooley D. M. (2000) Towards the development f selective amine oxidase inhibitors mechanism-based inhibition of six copper containing amine oxidases. *Eur. J. Biochem*. 269, 3645-3658.

Shimizu, E., Odawara, T., Tanizawa, K., and Yorifuji, T. (1994) Histamine oxidase, a quinoprotein enzyme of *Arthrobacter globiformis*. *Biosci. Biotech. Biochem.* 58(11), 2118-2120.

Simon, de Vries, Rob, J.M. van Spanning, and Vincent steinebach (2000) A spectroscopic and kinetic study of *Escherichia coli* amine oxidase. *Journal of molecular catalysis B: Enzymatic* 8, 111-120.

Steinnebach, V., Vries, S. D., and Duine J. A. (1996) Intermediates in the catalytic cycle of copper-quinonprotein amine oxidase from *Escherichia coli*. *J. Biol. Chem.* 271, 5580-5588.

Stites T. E., Mitchell A. E., and Rucker R. B. (2000) Physiological Importance of Quinoenzymes and the *O*-Quinone Family of Cofactor, *J. Nutr.* 130, 719-727.

Stoner P. (1985) An improved spectrophotometric assay for histamine and diamine oxidase (DAO) activity. *Agents Action*s, 17, 5-9.

Wilce, M. C. J., Dooley, D. M., Freeman, H. C., Guss, J. M., Matsunami H., William, S. M., Ruggiero, C. E., Tanizawa, K., and Yamaguchi, H. (1997) Crystal structure of the copper-containing amine oxidase from *Arthrobacter globiformis* in the holo and apo forms:

implications for the biogenesis of topaquinone. *Biochemistry* 36,16116-16133.

Wilmot, C. M., Murray, J. M., Alton, G., Parsons, M. R., Convery, M. A., Blakeley, V., Corner, A. S. Palcic, M. M., Knowles, P. F., McPherson, M. J., and Philips, S. E. V. (1997) Catalytic mechanism of the quinonenzyme amine oxidase from Escherichia coli: exploring the reductive half-reaction. *Biochemistry* 36, 1608-1620.

Shimizu E., Odawara T., Tanizawa K., and Yorifuji T. (1994) Histamine oxidase, a Cu^{2+}-quinoprotein enzyme of *Arthrobacter globiformis*. *Biosci. Biotech. Biochem.* 58(11), 2118-2120.

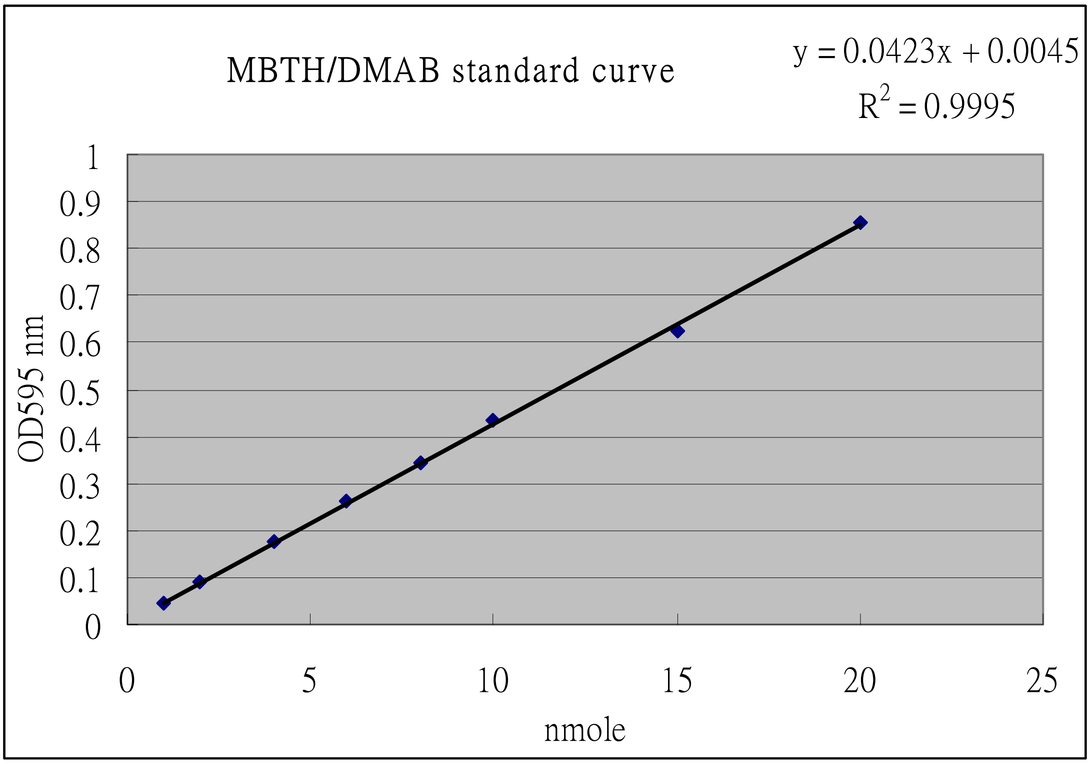

Figure 1 H_2O_2 standard curve

The procedure is the same with activity assay except that amine oxidase and substrates were replaced with H_2O_2 in amounts from 1.0 to 20 nmole.

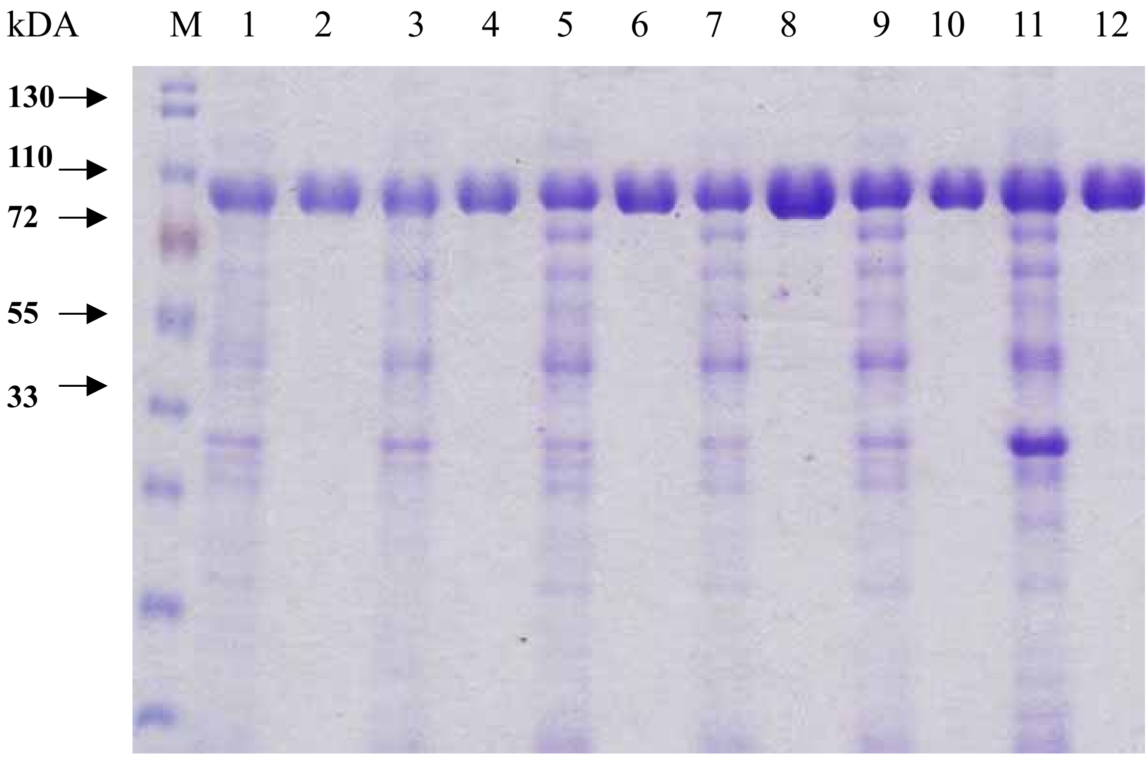

Figure 2 10% SDS-PAGE of crude extract and purified AGHO and mutants

The crude extracts and purified wild type AGHO (5 μg) and its mutants (5 μg) were separated on a 10 % SDS-PAGE and stained with Comassie Blue. *M*: molecular weight standards (MBI Marker): 130, 110, 72, 55, and 33 kDa. *Lane 1, 2*: crude extract of Cu^{2+}-free inactive form AGHO and its purified protein. *Lane 3, 4*: crude extract of Cu^{2+}-free inactive Y316A mutant and its purified protein. *Lane 5, 6*: crude extract of Cu^{2+}-free inactive Y316E mutant and its purified protein. *Lane 7, 8*: crude extract of Cu^{2+}-free inactive Y316F mutant and its purified protein *Lane 9, 10*: crude extract of Cu^{2+}-free inactive Y316H mutant and its purified protein. *Lane 11, 12*: crude extract of Cu^{2+}-containing active AGHO and its purified protein.

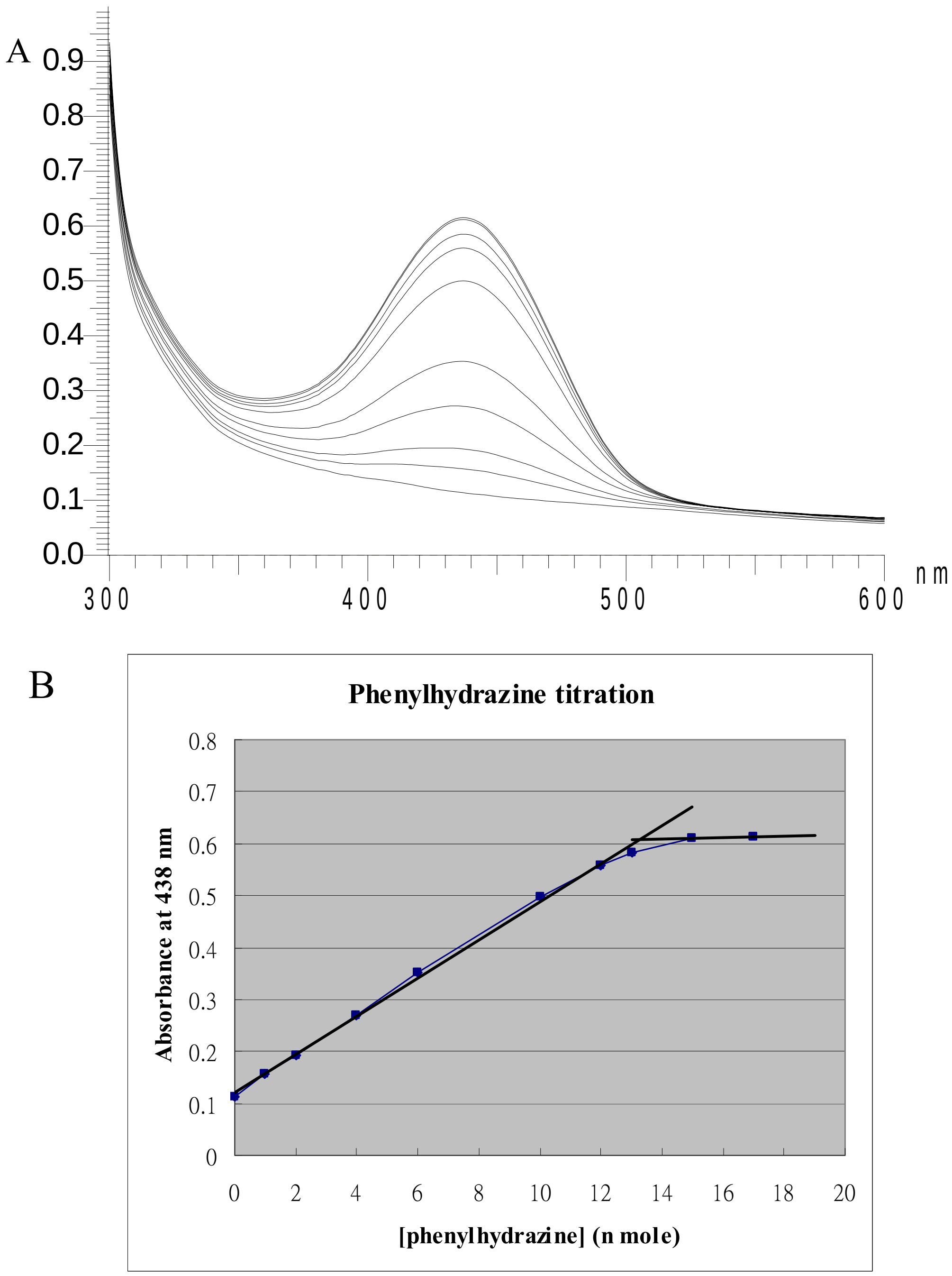

Figure 3 Phenylhydrazine titration of TPQ in AGHO.

A: The change in absorbance at 438nm versus equivalents phenylhydrazine added per enzyme dimer. Purified enzyme (12.5 nmole enzyme in 50 mM potassium phosphate buffer, pH 7.0) titrated with 0, 1, 2, 4, 6, 10, 12, 13, 15, and 17 nmole phenylhydrazine. B: The increase in absoption of the intensely yellow-colored adducts with successive phenylhydrazine additions.

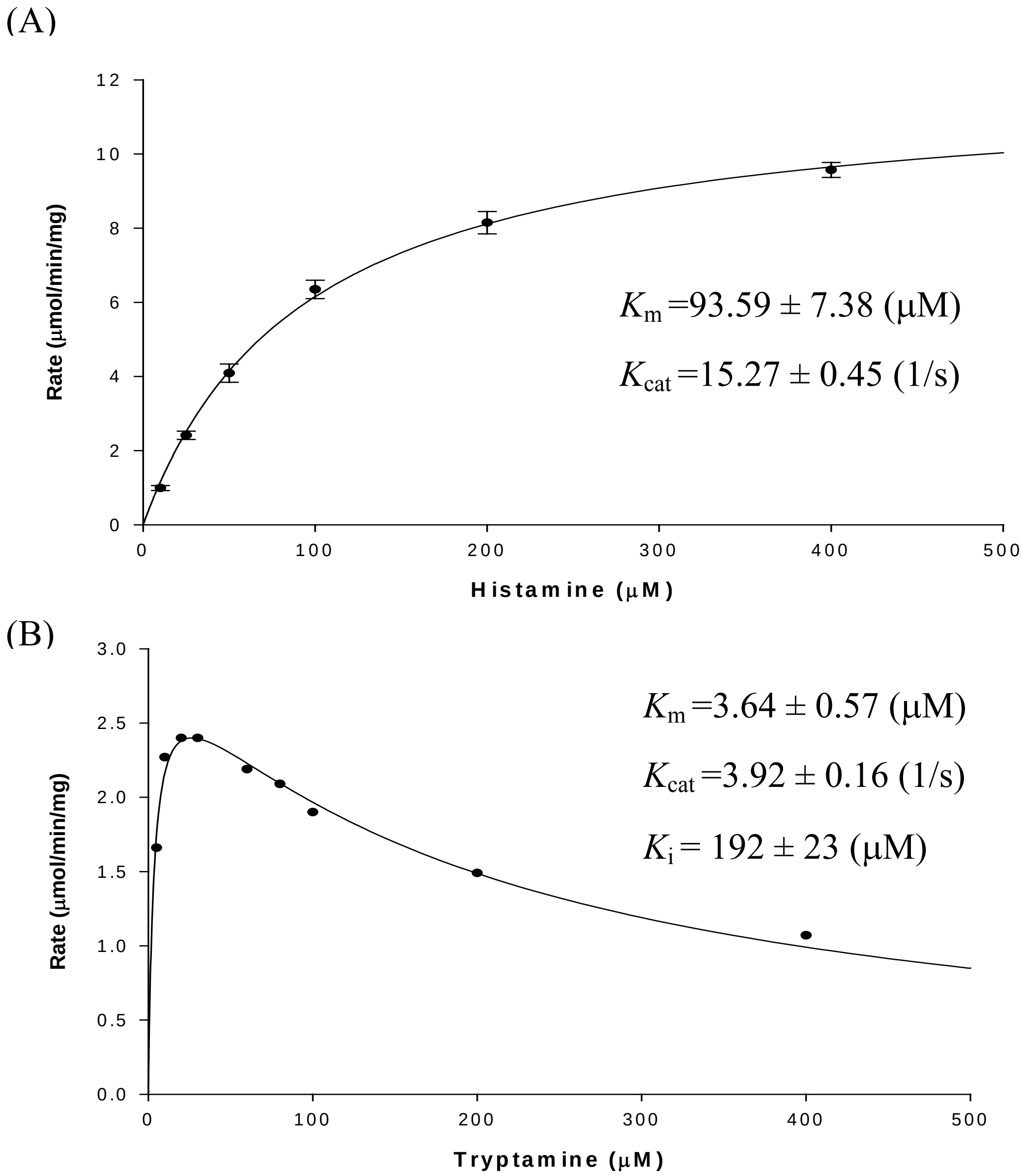

Figure 4 Plots of initial rate vs. substrate concentrations, demonstrating substrate inhibition observed with wild type AGHO.

(A) Plot of initial rate vs. concentration of Histamine

Various concentration of Histamine (0, 10, 25, 50, 100, 200, 400 μM) were used to find out the initial rate at each concentration. Results were the means±S.D. from three separate experiments, each carried out in triplicate.

(B) The initial rate of AGHO at each concentration of Tryptamine (0, 5, 10, 20, 30, 60, 80, 100, 200, 400 μM) were elucidated.

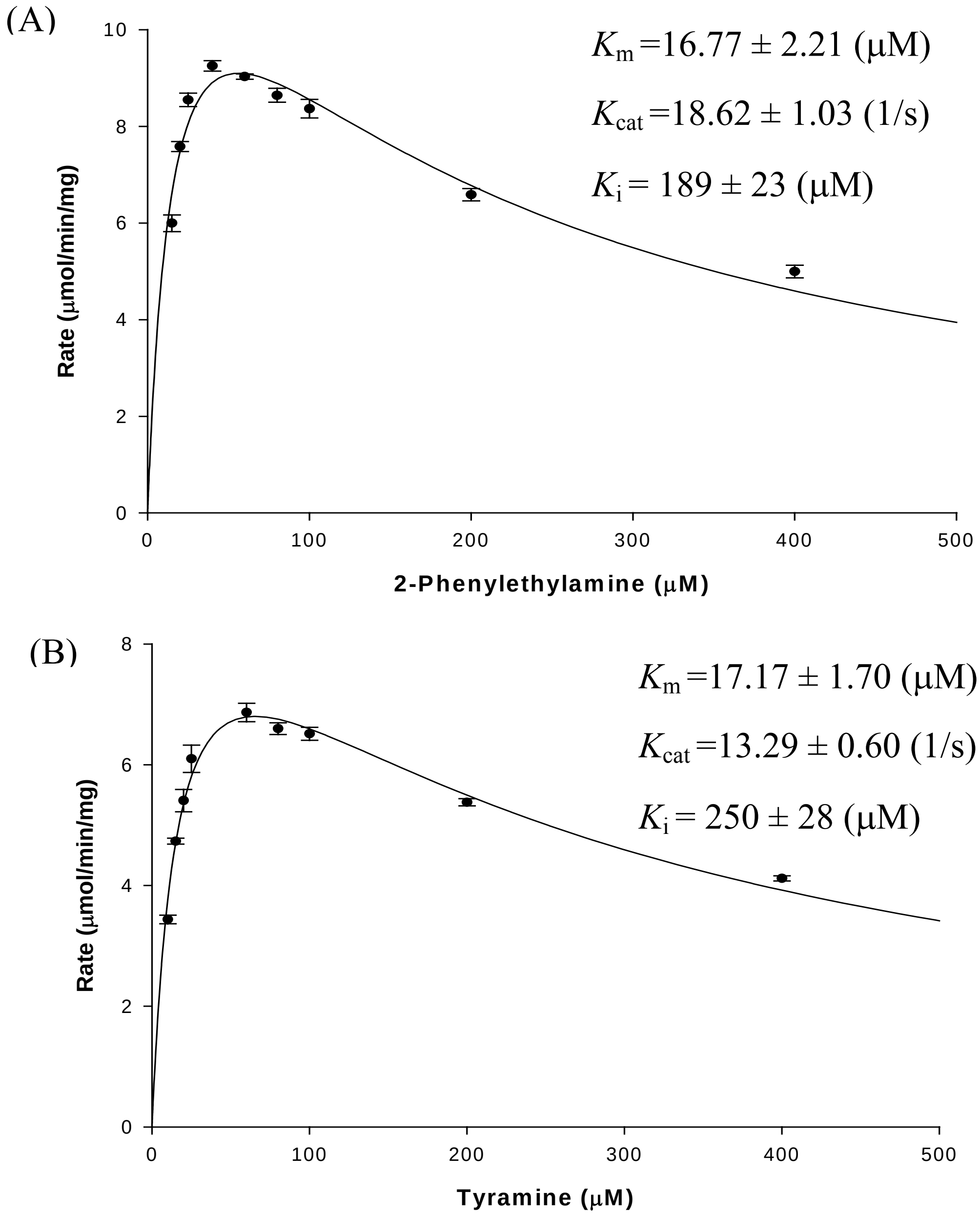

Figure 5 Plots of initial rates vs. substrate concentration

(A) Initial rate vs. concentration of β-phenylethylamine

Various concentration of β-phenylethylamine (0, 15, 20, 25, 40, 60, 80, 100, 200, 400 μM) were to find out the initial rate at each concentration.

(B) The initial rate of AGHO at each concentration of Tyramine (0, 10, 15, 20, 25, 60, 80, 100, 200, 400 μM) were elucidated.

Results were the means±S.D. from three separate experiments, each carried out in triplicate.

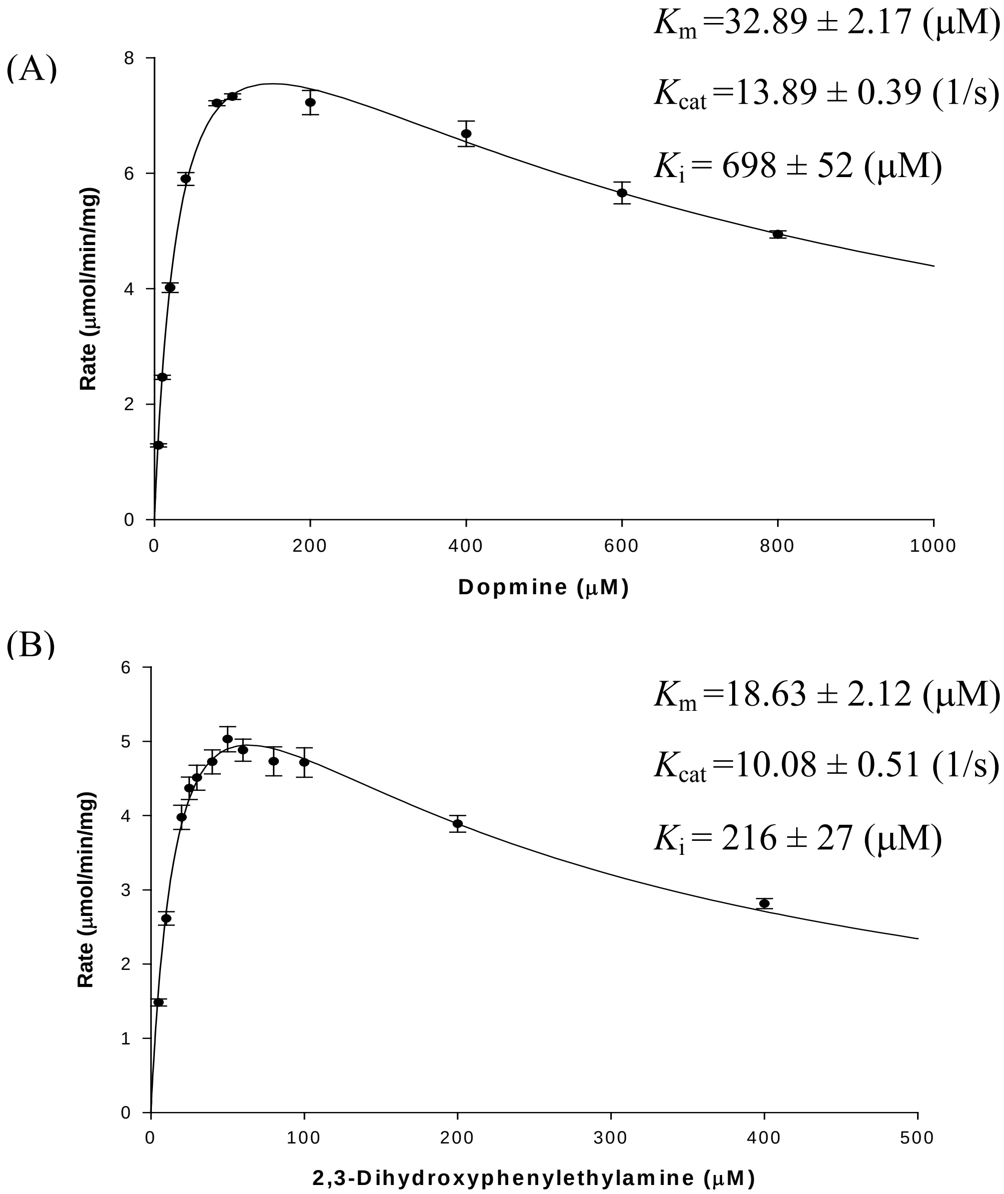

Figure 6 Plots of initial rates vs. substrate concentrations

(A) Initial rate vs. concentration of Dopamine

Various concentration of Dopamine (0, 5, 10, 20, 40, 80, 100, 200, 400, 600, 800 μM) were to find out the initial rate at each concentration.

(B) The initial rate of AGHO at each concentration of 2, 3-Dihydroxyphenylethylamine (0, 5, 10, 20, 25, 30, 40, 50, 60, 80, 100, 200, 400 μM) were elucidated.

Results were the means±S.D. from three separate experiments, each carried out in triplicate.

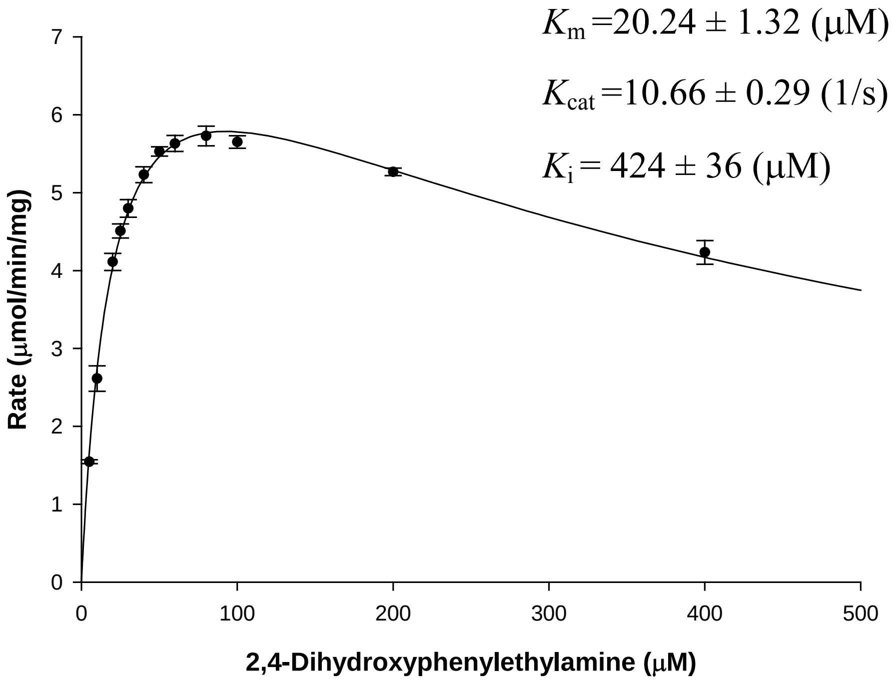

Figure 7　Plots of initial rates vs. substrate concentrations

Initial rate vs. concentration of 2, 4-Dihydroxyphenylethylamine

Various concentration of 2, 4-Dihydroxyphenylethylamine (0, 5, 10, 20, 25, 30, 40, 50, 60, 80, 100, 200, 400 μM) were to find out the initial rate at each concentration.

Results were the means ± S.D. from three separate experiments, each carried out in triplicate.

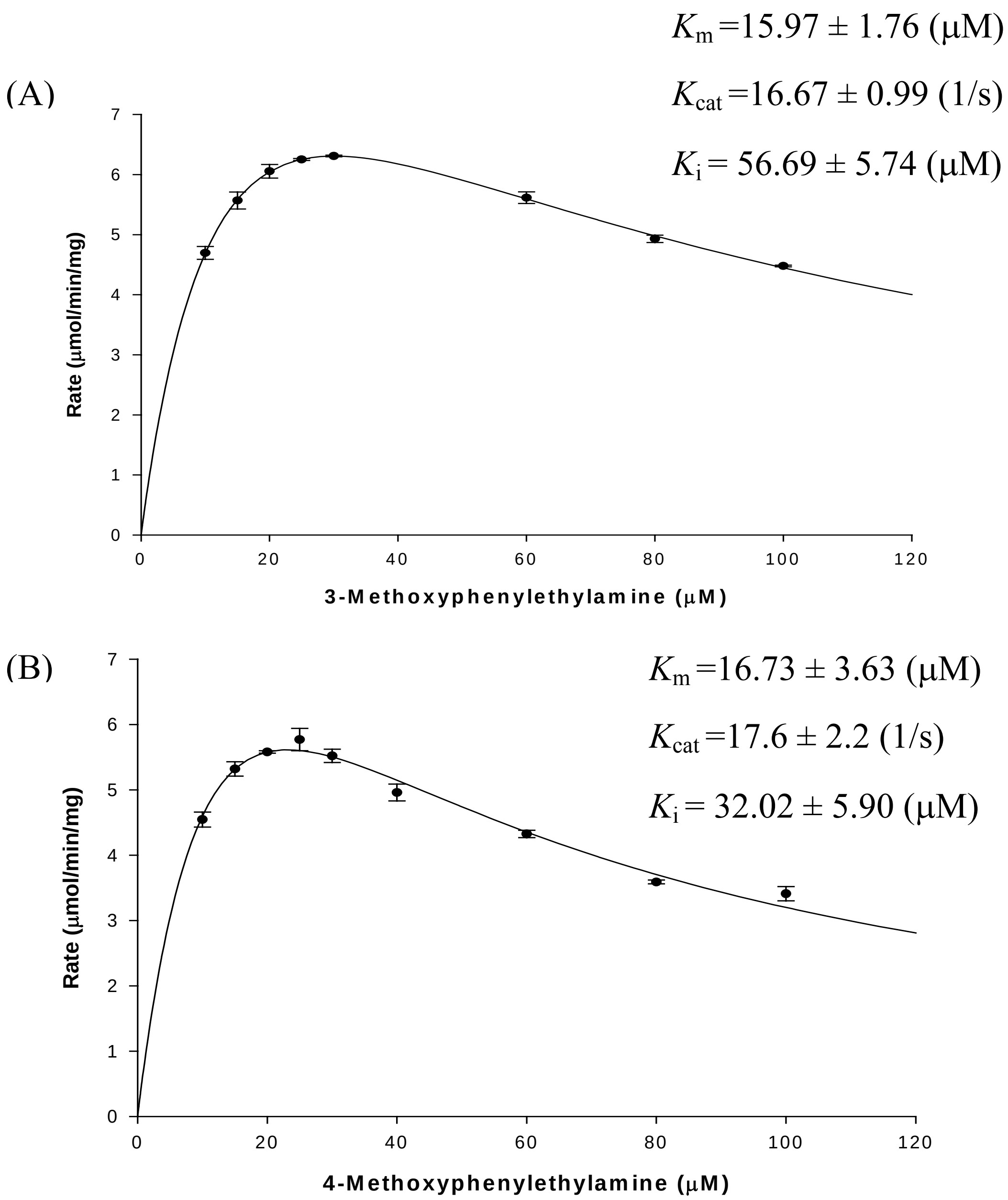

Figure 8 Plots of initial rates vs. substrate concentrations

(A) Initial rate vs. concentration of 3-methoxyphenylethylamine

Various concentration of 3-methoxyphenylethylamine (0, 10, 15, 20, 25, 30, 60, 80, 100 μM) were to find out the initial rate at each concentration.

(B) The initial rate of AGHO at each concentration of 4-methoxyphenylethylamine (0, 10, 15, 20, 25, 30, 40, 60, 80, 100 μM) were elucidated.

Results were the means±S.D. from three separate experiments, each carried out in triplicate.

(A)

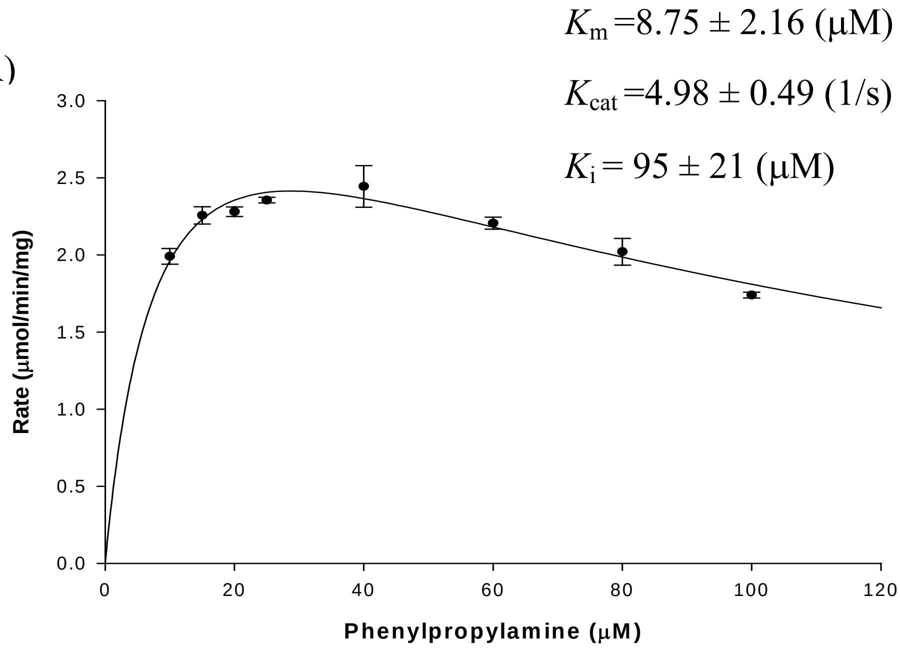

(B)

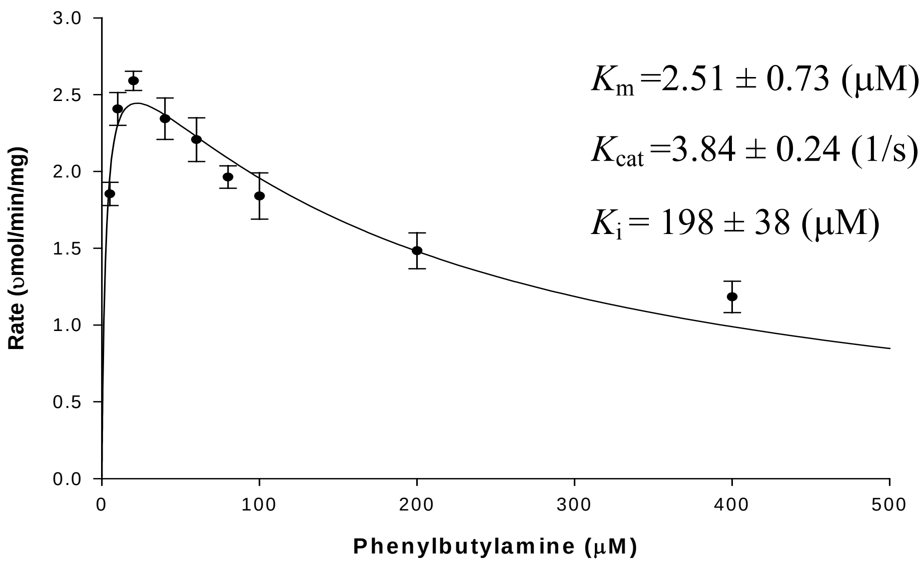

Figure 9 Plots of initial rates vs. substrate concentrations

(A) Initial rate vs. concentration of phenylpropylamine

Various concentration of phenylpropylamine (0, 10, 15, 20, 25, 40, 60, 80, 100 μM) were to find out the initial rate at each concentration.

(B) The initial rate of AGHO at each concentration of phenylbutylamine (0, 2.5, 5, 10, 20, 40, 60, 80, 100, 200, 400 μM) were elucidated.

Results were the means±S.D. from three separate experiments, each carried out in triplicate.

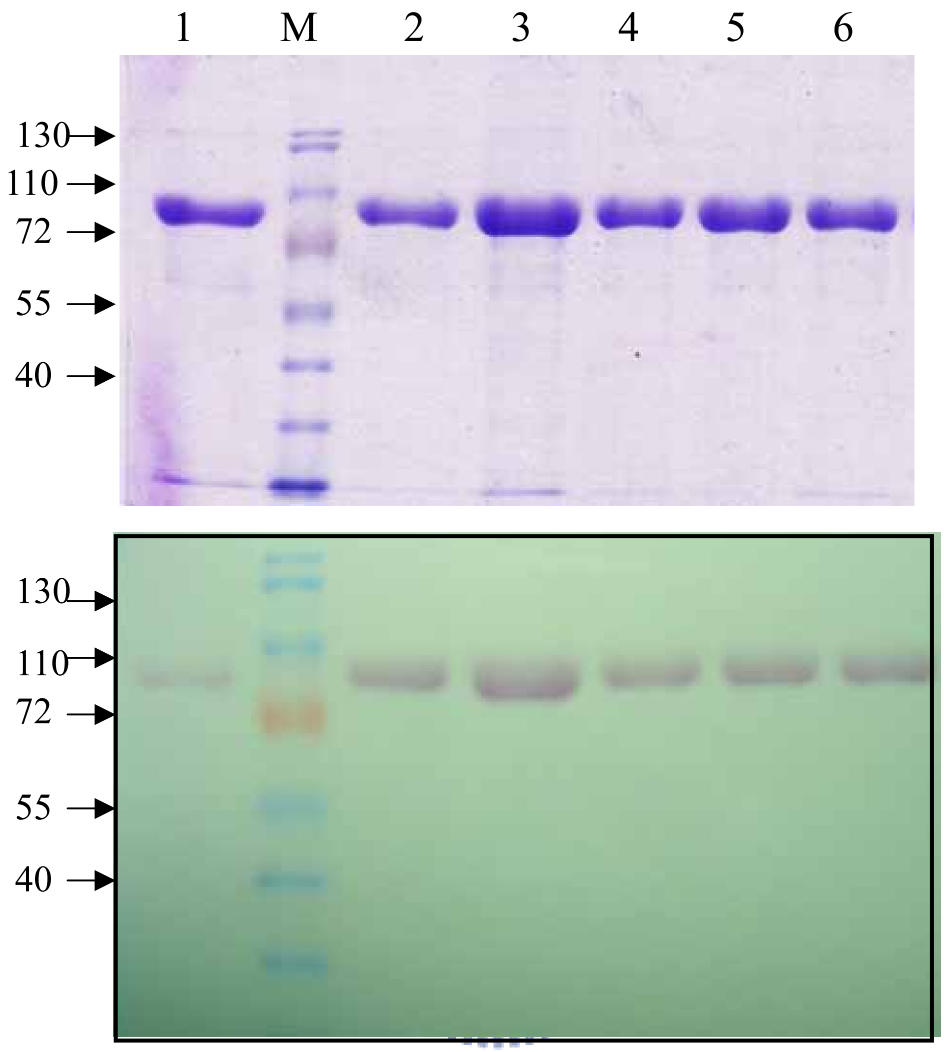

Figure 8　SDS-PAGE and NBT/Glycinate staining of wild-type and Y316 mutants of AGHO.

The samples were separated on 10% SDS-PAGE. M: molecular weight standards: 110, 72, 55, 40, and 33 kDa. *Lane 1* Cu^{2+}-free inactive form of AGHO. *Lane 2*: Cu^{2+} reconstituted activated form of AGHO[a]. *Lane3*: Y316A mutant[a] (8 μg). *Lane 4*: Y316E mutant[a]. *Lane 5*: Y316F mutant[a]. *Lane 6*: Y316H mutant[a]. The result presented is the representative of three separated experiments.

[a] after 50 μM $CuSO_4$ incubation at 30℃

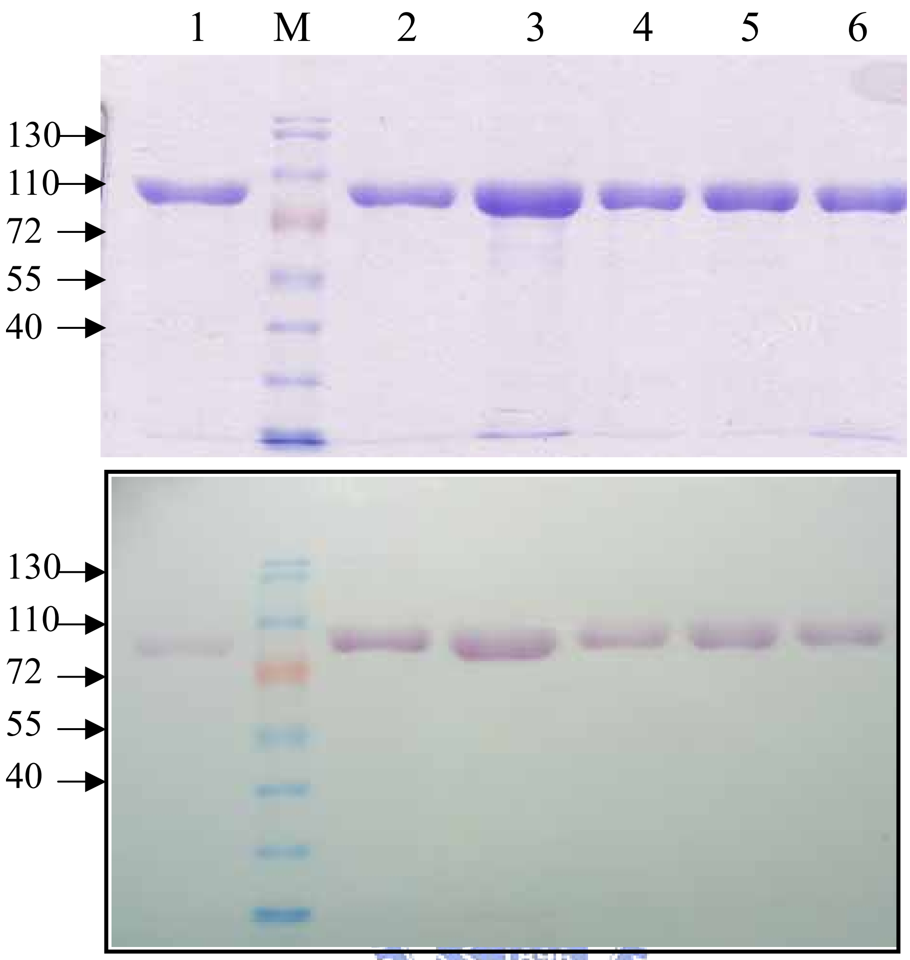

Figure 9 SDS-PAGE and NBT/Glycinate staining of wild-type and Y316 mutants of AGHO.

The samples were separated on 10% SDS-PAGE. M: molecular weight standards: 130, 110, 72, 55, 40, and 33 kDa. *Lane 1* Cu^{2+}-free inactive form of AGHO. *Lane 2*: Cu^{2+} reconstituted activated form of AGHO[a]. *Lane3*: Y316A mutant[a] (8 μg). *Lane 4*: Y316E mutant[a]. *Lane 5*: Y316F mutant[a]. *Lane 6*: Y316H mutant[a]. The result presented is the representative of three separated experiments.

[a] after 1 mM $CuSO_4$ incubation at 30℃

Step	Total protein (mg)	Total Activ. (U)[a]	Spec. Activ. (U/mg)[a]	Yield (%)	Purification fold (X)
Crude extract	**70.8**	**137.4**	**1.94**	**100**	**1**
Dialysis after ammonia sulfate (0-50%)	**18.5**	**70.3**	**3.8**	**51**	**1.95**
His-Tag affinity purification	**7.8**	**52.5**	**6.73**	**38**	**3.46**

Table 1　Purification table of Cu^{2+}-free in active form of AGHO

[a] The activity was determined after incubation with 50 μM $CuSO_4$ at 30℃ for 30 min.

(I) 50 mM $CuSO_4$ activated

Enzyme	Wild-type (A)	Wild-type (B)	Y316A	Y316E	Y316F	Y316H
Specific Activ. (U)	6.76	5.46	ND	ND	1.66	ND

(II) 1 mM CuSO4 activated

Enzyme	Wild-type (A)	Wild-type (B)	Y316A	Y316E	Y316F	Y316H
Specific Activ. (U)	6.82	5.58	ND	ND	1.28	ND

Enzyme	Wild-type	Y316A	Y316E	Y316F	Y316H
Histamine	6.73	ND	ND	1.28	ND
Phenylethylamine	9.33	ND	ND	3.4	ND
Methylamine	ND	ND	ND	ND	ND
Ethylamine	ND	ND	ND	ND	ND

Table 2 The specific activity summary of Cu^{2+}-containing active (B) wild-type enzyme and Cu^{2+}-reconstituted wild-type (A) and Y316 mutant enzymes.

The activity was determined after incubation with 50 μM $CuSO_4$ at 30℃ for 30 min. All substrate concentration were 100 μM

ND: Undetectable

Table 3 Relative activity toward aliphatic and aromatic amines

Relative reaction rate of AGHO reacted with various substrates	
Substrate	Relative activity (%)
Histamine	100
Tryptamine	25
Benzylamine	0.5
2-Phenylethylamine	154
3-Phenylpropylamine	40
4-Phenylbutylamine	28
Tyramine	107
2,3-Dihydroxyphenylethylamine	84
2,4-Dihydroxyphenylethylamine	80
3,4-Dihydroxyphenylethylamine (Dopamine)	125
3-Methoxy-phenylethylamine	67
4-Methoxy-phenylethylamine	55
Serotonin	12
Norepinephrine	4
Methylamine	-
Ethylamine	-
4-Aza-1, 8-diaminooctane (Spermidine)	-
4,9-Diaza-1, 12-diaminododecane (Spermine)	-

The negative symbol (-) denotes that substrate oxidation rate was too slow to determine it under our activity assay condition.

Amine	K_m (μM)	K_{cat} (S^{-1})	K_{cat} (μM)	K_{cat}/K_m ($\mu M^{-1}S^{-1}$)
Histamine	93.59 ± 7.38	15.27 ± 0.45	-	0.16
Tryptamine	3.64 ± 0.57	3.92 ± 0.16	192 ± 23	1.08

Table 4 Comparison of K_{cat}, K_{cat}/K_m, K_m Values for imidole-structure amines

The initial rate of oxidation of tryptamine was determined with a 60 sec reaction.

Results were the means±S.D. from three separate experiments, each carried out in triplicate.

Amine	K_m (μM)	K_{cat} (S^{-1})	K_i (μM)	K_{cat}/K_m ($\mu M^{-1}S^{-1}$)
Phenylethylamine	16.77 ± 2.21	18.62 ± 1.03	188 ± 23	1.11
Tyramine	17.17 ± 1.70	13.29 ± 0.60	250 ± 28	0.77
2,3-Dihydroxyphenylethylamine	18.63 ± 2.12	10.08 ± 0.51	216 ± 27	0.54
2,4-Dihydroxyphenylethylamine	20.24 ± 1.32	10.66 ± 0.29	424 ± 36	0.53
3,4-Dihydroxyphenylethylamine (Dopamine)	32.89 ± 2.17	13.89 ± 0.39	698 ± 52	0.42
3-Methoxy-phenylethylamine	15.97 ± 1.76	16.67 ± 0.99	56.7 ± 5.74	1.04
4-Methoxy-phenylethylamine	16.73 ± 3.63	17.60 ± 2.20	32.2 ± 5.90	1.05
DL-Octopamine	122.10 ± 5.08	3.95 ± 0.06	-	0.03

Table 5　Comparison of K_{cat}, K_{cat}/K_m, K_m Values for different functional group substituted on the ring of aromatic amines

Results were the means ± S.D. from three separate experiments, each carried out in triplicate

Amine	K_m (μM)	K_{cat} (S^{-1})	K_i (μM)	K_{cat}/K_m ($\mu M^{-1}S^{-1}$)
Benzylamine	-[a]	-	-	-
Phenylethylamine	16.77 ± 2.21	18.62 ± 1.03	188.64 ± 23.36	1.11
Phenylpropylamine	8.75 ± 2.16	4.98 ± 0.49	94.5 ± 20.6	0.57
Phenylbutylamine	2.50 ± 0.73	3.84 ± 0.24	197.8 ± 37.6	1.53

Table 6 Comparison of K_{cat}, K_{cat}/K_m, K_m Values for different aliphatic chain length of aromatic amines

Results were the means ± S.D. from three separate experiments, each carried out in triplicate

[a]The dash (-) denotes substrate oxidation could be detected, but the catalytic rate is too low to carry kinetic study.

The initial rate of oxidation of phenylpropylamine was determined by a 60 sec reaction time period.

Appendix 1　Amine list

Name	Structure
Histamine Synonyms: 2-(4-Imidazolyl)ethylamine Molecular Formula: $C_5H_9N_3$ Molecular Weight: 111.1	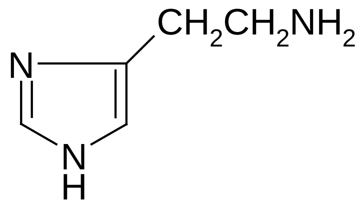
1-Methylhistamine-dihydrochloride Synonyms: 1-Methyl-4-(β-aminoethyl)imidazole Dihydrobromide Molecular Formula: $C_6H_{11}N_3 \cdot 2HCl$ Molecular Weight: 198.1	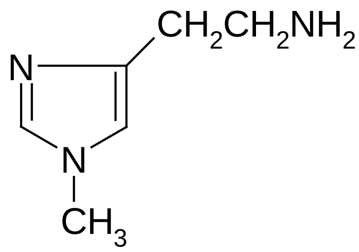
Serotonin-hydrochloride Synonyms: (5-hydroxytryptamine hydrochloride) Molecular Formula: $C_{10}H_{12}N_2O \cdot HCl$ Molecular Weight: 212.68	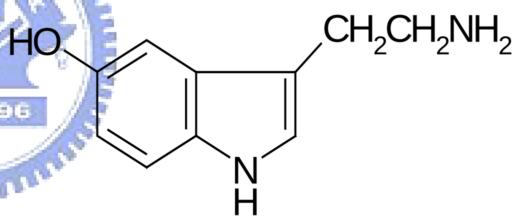
Tryptamine Synonyms: 3-(2-aminoethyl)indole Molecular Formula: $C_{10}H_{12}N_2$ Molecular Weight: 160.22	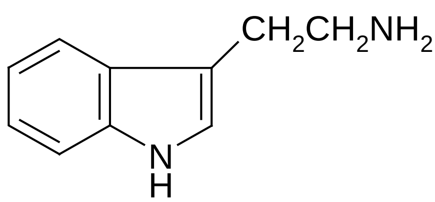
Amphetamine(Benzedrine) Molecular Formula: $C_9H_{13}N_1$ Molecular Weight: 135	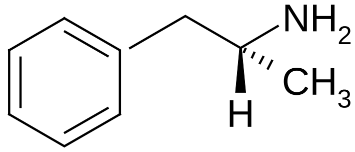

Benzylamine Molecular Formula: $C_6H_5CH_2NH_2$ Molecular Weight: 107.16	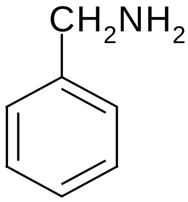
beta-Phenylethylamine Synonyms: 2-Phenylethylamine Molecular Formula: $C_8H_{11}N$ Molecular Weight: 121.2	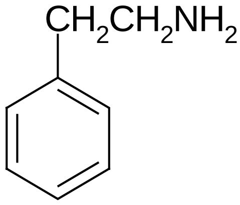
beta-Phenylethylamine Synonyms: 2-Phenylethylamine Molecular Formula: $C_8H_{11}N$ Molecular Weight: 121.2	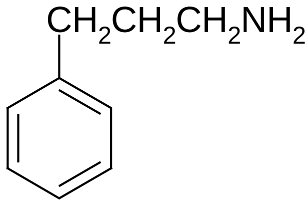
beta-Phenylethylamine Synonyms: 2-Phenylethylamine Molecular Formula: $C_8H_{11}N$ Molecular Weight: 121.2	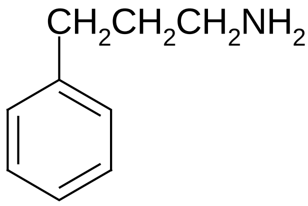
Tyramine Synonyms: 4-(2-Aminoethyl)phenol- 4-Hydroxyphenethylamine Tyrosamine Molecular Formula: $C_8H_{11}NO$ Molecular Weight: 137.2	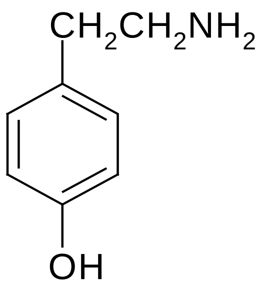
Dopamine-hydrochloride Synonyms: 3-Hydroxytyramine hydrochloride Molecular Formula: $C_8H_{11}NO_2 \cdot HCl$ Molecular Weight: 189.6	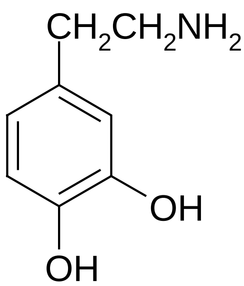

2,3-dihydroxyphenylethylamine Molecular Formula: $C_8H_{11}NO_2$ Molecular Weight: 169.2	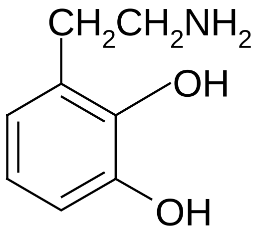
2,4-dihydroxyphenylethylamine Molecular Formula: $C_8H_{11}NO_2$ Molecular Weight: 169.2	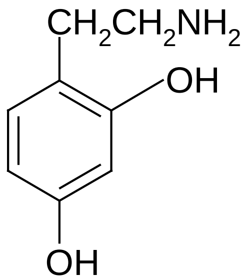
(-)- Noreprinephrine Synonyms: L-Arterenol Molecular Formula: $C_8H_{11}NO_3$ Molecular Weight: 169.2	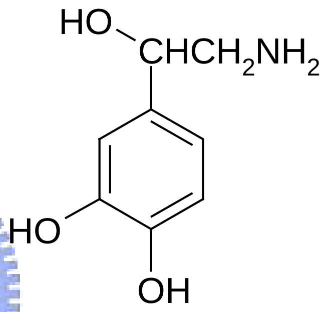
Epinephrine Synonyms: L-Adrenaline Molecular Formula: $C_9H_{13}NO_3$ Molecular Weight: 183.2	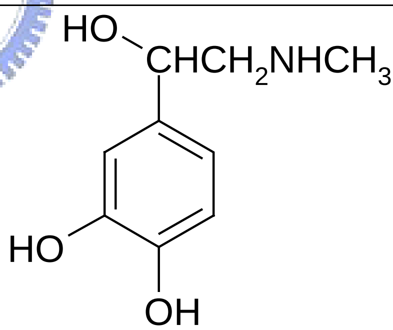

Aliphatic amine：

Methylamine Synonyms: Monomethylamine. Molecular Formula: CH_5N Molecular Weight: 31.06	CH_3NH_2
Ethylamine Synonyms: Ethanamine Molecular Formula: C_2H_7N Molecular Weight: 45.08	$CH_3CH_2NH_2$
1,4-Diaminobutane Synonyms: Putrescine Molecular Formula: $C_4H_{12}N_2$ Molecular Weight: 88.15	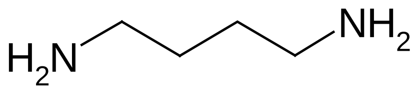
1,5-Diaminopentane Synonyms: Cadaverine Molecular Formula: $C_5H_{14}N_2$ Molecular Weight: 102.2	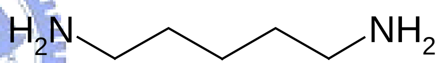
Spermine Synonyms: N,N'-Bis(3-aminopropyl)-1,4-diaminobutane Molecular Formula: $C_{10}H_{26}N_4$ Molecular Weight: 202.3	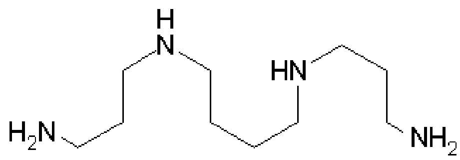
Spermidine Synonyms: 1,8-Diamino-4-azaoctane Molecular Formula: $C_7H_{19}N_3$ Molecular Weight: 145.2	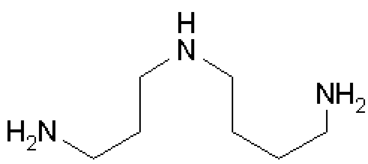

Appendix 2 Plasmids and vectors used in the work

Number	Name	Origin
1	**pUC-T/ AGHO-I (S134A+Y316A)**	**Lin Y. H., 2002**
2	**pUC-T/ AGHO-I (S134A+Y316E)**	**This project**
3	**pUC-T/ AGHO-I (S134A+Y316F)**	**This project**
4	**pUC-T/ AGHO-I (S134A+Y316H)**	**Lin Y. H., 2002**
5	**pET30(-S)/AGHO**	**Chang S. P., 2003**
6	**pET30(-S)/AGHO(V586G)**	**Chang S. P., 2003**
7	**pET30b(-S)/AGHO (Y316A)**	**This project**
8	**pET30b(-S)/AGHO (Y316E)**	**This project**
9	**pET30b(-S)/AGHO (Y316F)**	**This project**
10	**pET30b(-S)/AGHO (Y316H)**	**This project**

Appendix 3 Primers of Site-directed mutagenesis

primer	**Sequence (from 5' end to 3' end)**
AGHO Y316E/ L	**5:GCTGGCAGAACGAATTCGACTCCGG:3**
AGHO Y316E/ R	**5:CCGGAGTCGAATTCGTTCTGCCAGC:3**
AGHO Y316F/ L	**5:GCTGGCAGAACTTCTTCGACTCCGG:3**
AGHO Y316F/ R	**5:CCGGAGTCGAAGAAGTTCTGCCAGC:3**

Appendix 4 TPQ biogenesis

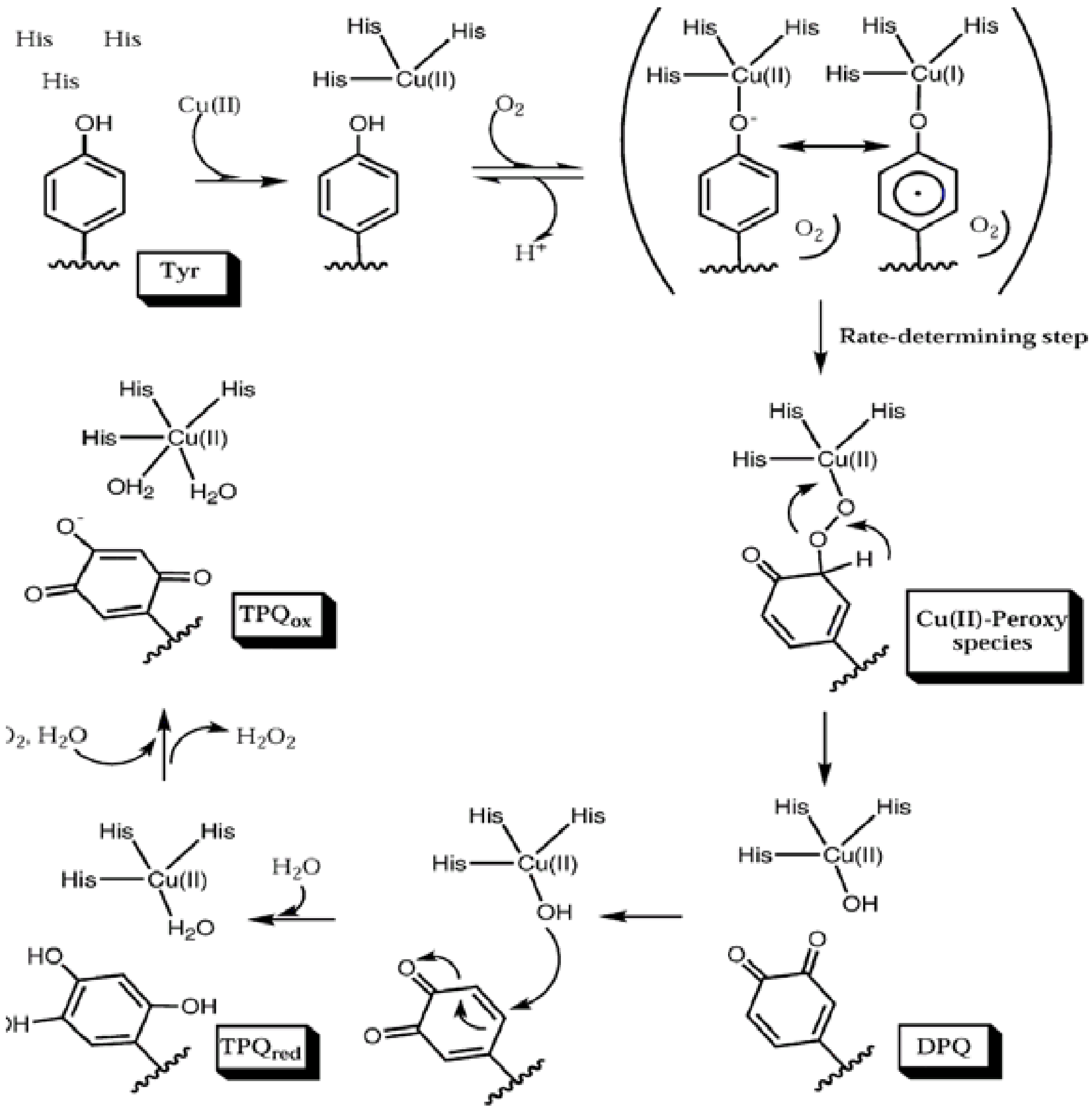

Prabhakar, R. (2004), J.Am.Chem.Soc.

The mechanism is divided into six steps. At first, copper binds anaerobically to the enzyme. Second, dioxygen binds at a site near the precursor tyrosine. Dioxygen is proposed to react with the Cu (II)-tyrosinate species and form a bridging peroxy intermediate in the suggested third step, and then the DPQ ring first rotates 180° around the Cβ-Cγ bond so that the C-2 position of TPQ faces the Cu metal center in the suggested fourth step. In this position, it is set up for a nucleophilic attack by a copper-coordinated water or hydroxide. In the suggested fifth step, the C-2 site of TPQ is oxidized. In the final step of the mechanism, dioxygen enters, and hydrogen peroxide is formed. (Prabhakar *et al.*, 2004)

Appendix 5   Catalytic cycle

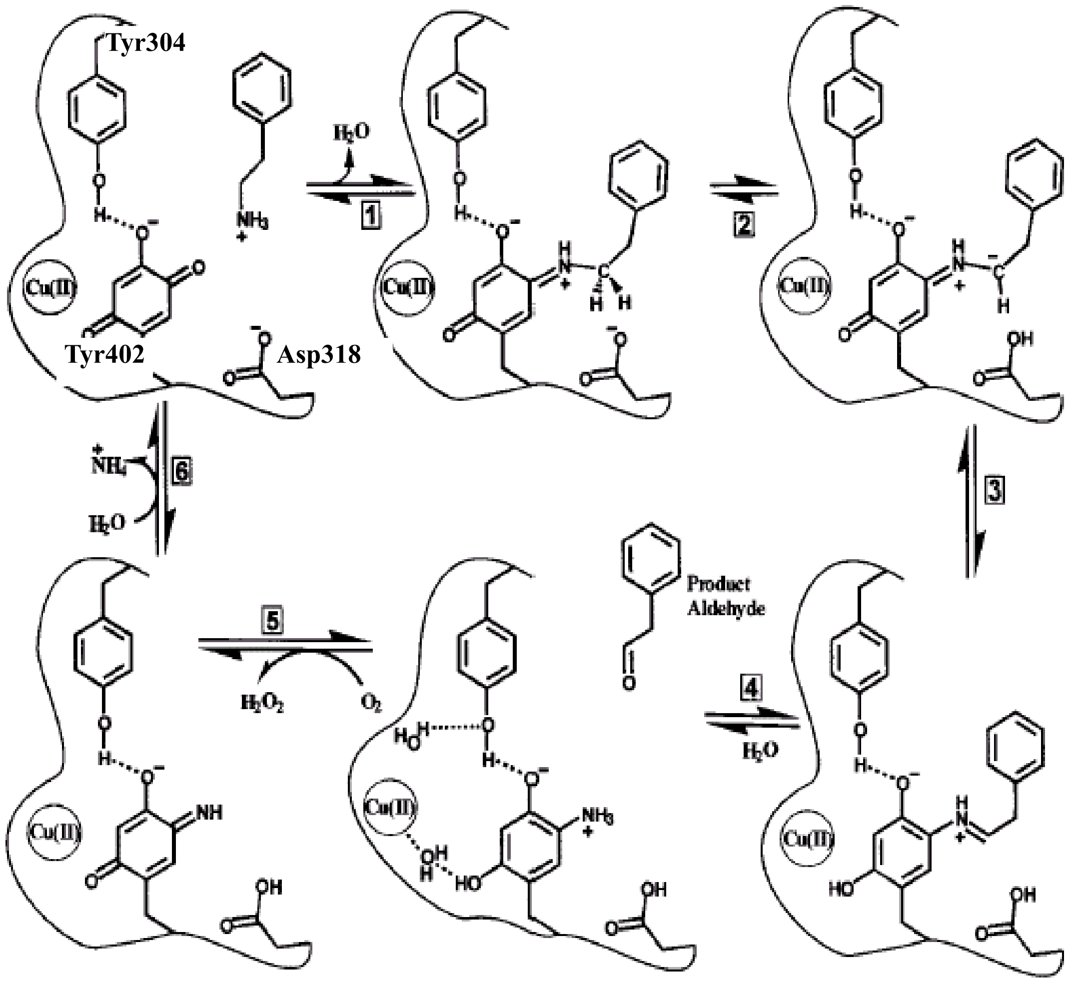

The substrate is deprotonated and forms the substrate Schiff base with TPQ_{ox}(step 1). A hydrogen is abstracted, by Asp318 in AGHO, from the methylene group (step 2), allowing rearrangement to the product Schiff base (step 3). Product aldehyde is released by hydrolysis to leave reduced enzyme (step 4); some hydrogen bonds associated with the reduced (aminoquinol) TPQ are shown by dashed lines. Oxygen, the second substrate, binds to the enzyme and is reduced to hydrogen peroxide (step 5), giving iminoquinone with subsequent hydrolysis and release of ammonia, regenerating the active enzyme (step 6). (Murray *et al.*, 2001)

Appendix 6 Plasmid map

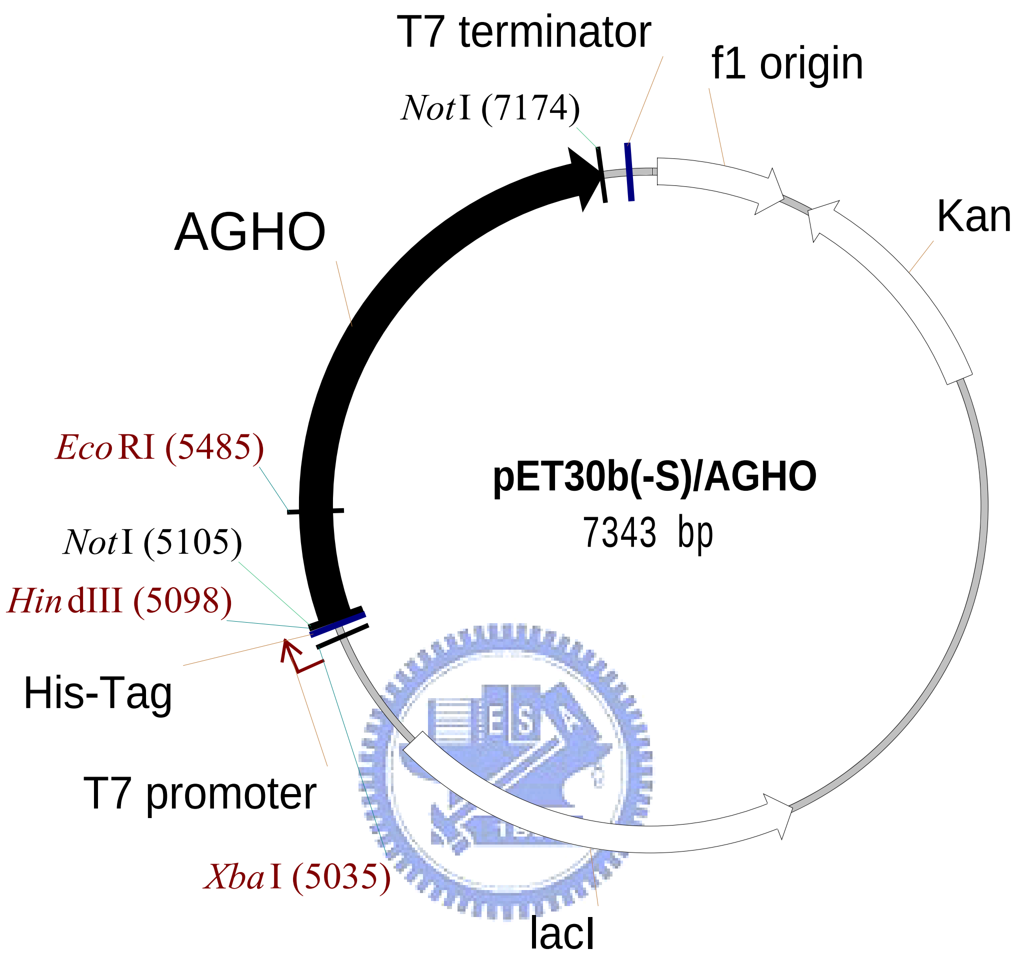

Appendix 7 Sequence alignment

```
01-AGHO  : RPVIHRASISEMVVPYGDPSPYRSWQNYFDSGEYLVGRDANSLRLGCDCLGDIT : 341
02-AGPEO : RPIINRASIAEMVVPYGDPSPIRSWQNYFDTGEYLVGQYANSLELGCDCLGDIT : 322
03-AGMO1 : RPVINRASLSEMVVPYGDTAPVQAKKNAFDSGEYNIGNMANSLTLGCDCLGEIK : 325
04-AGMO2 : RPVINRASLSEMVVPYGDTAPVQAKKNAFDSGEYNIGNMANSLTLGCDCLGEIK : 325
05-ANAO  : RSVLYRLSVSEMTVPYADPRPPFHRKQAFDFGDGGGGNMANNLSIGCDCLGVIK : 345
06-ECAO  : RKVMYEGSLGGMIVPYGDPDIGWYFKAYLDSGDYGMGTLTSPIARGKDAPSNAV : 437
07-KAMO  : RQVMYEGSLGGMIVPYGDPDVGWYFKAYLDSGDYGMGTLTSPIVRGKDAPSNAV : 437
08-HPAO  : RPIFHRISLSEMIVPYGSPEFPHQRKHALDIGEYGAGYMTNPLSLGCDCKGVIH : 343
09-LSAO  : RRVLYKGYISELFVPYQDPTEEFYFKTFFDSGEFGFGLSTVSLIPNRDCPPHAQ : 342
10-PSAO  : RRVLYKGYISELFVPYQDPTEEFYFKTFFDSGEFGFGLSTVSLIPNRDCPPHAQ : 349
11-HABP  : ERIAYEVSVQEAVALYGGHTPAGMQTKYLDVG-WGLGSVTHELAPGIDCPETAT : 396
12-HRAO  : ERIAYEVSVQECVSIYGADSPKTMLTRYLDSS-FGLGRNSRGLVRGVDCPYQAT : 403
13-HVAP1 : ERLVYEISLQEALAIYGGNSPAAMTTRYVDGG-FGMGKYTTPLTRGVDCPYLAT : 409
14-BLAO1 : ERLAYEISLQEAGAVYGGNTPAAMLTRYMDSG-FGMGYFATPLIRGVDCPYLAT : 408
15-BLAO2 : ERLAYEISLQEAVAIYGGNTPAAMLTRYMDAC-FGMGKFATPLTRGVDCPYLAT : 408
16-RAAO  : ERVAYEVSVQEAVALYGGHTPAGMQTKYIDVG-WGLGSVTHELAPGIDCPETAT : 391
17-MVAP1 : ERVAYEISVQEAIALYGGNSPASMSTCYVDGS-FGIGKYSTPLIRGVDCPYLAT : 409
             6    s6 e    Yg            D g    G     6  g Dc
```

Chang S. P., 2003